Al-Nahrain Journal of Science
ANJS, Vol.28 (4), December, 2025, pp. 83-113

Graphene Nanoplatelets Applied as Functional Fillers in Self-Sensing Engineered Cementitious Composites ECC Matrix

Shatha Riyadh Ahmed*, Ali Majeed Al-Dahawi, Shatha Sadeq Hassan

[1] Civil Engineering Department, University of Technology, Baghdad, Iraq.

Article's Information

Received: 10.03.2025
Accepted: 08.12.2025
Published: 15.12.2025

Keywords:
Functional Additives,
Graphene Nanoplatelets (GNP),
Polyvinyl Alcohol Fibers (PVA),
Nylon Fibers (NF),
Electrical Resistivity (ER),
Self-Sensing of Damage,
Fractional Change in Electrical Resistivity (FCER).

Abstract

The widespread adoption of innovative cementitious composites requires proper attention to the controlled performance of structures by using these functional materials. This paper delves deeper into this concept, utilizing a conventional Engineered Cementitious Composites (ECC45) matrix that has been embedded with conductive fillers, enabling it to detect damage in a variety of loading scenarios. As functional fillers, graphene nanoplatelets (GNPs) combined with polyvinyl alcohol (PVA) and nylon (NF) fibers were used at different curing ages of 28, 56, 90, and 180 days. In an attempt to build on previous results and address some knowledge gaps, the simple matrix was incorporated with graphene nanoplatelets at a fixed concentration of 2 % by wt. of cementitious materials along with one of the reinforcement fibers (PVA) or (NF) at 2% volume fraction, which remained constant throughout the experiment. The matrices were tested for compressive strength, splitting strength, three-point flexural strength, and direct tensile strength to evaluate the innovative matrices' behavior and ability to sense damage under these types of stresses. results demonstrated a unique behavior of the samples due to the excellent behavior of GNPs, particularly during the late curing ages, and the synergistic behavior it exhibits with the reinforcement fibers, which enables entire additives to work in a balanced manner in developing the self-sensing ability in conjunction with the high efficiency of the mechanical properties against the loading conditions described in this paper.

http://doi.org/10.22401/ANJS.28.4.08
*Corresponding author: 11064@uotechnology.edu.iq

1. Introduction

Recently, the concept of cementitious composites has begun to transform from conventional composites to smart and advanced functional composites on both mechanical and electrical axes by integrating them with conductive fillers that make them useful in several applications, including self-sensing of loads imposed on the concrete structure under different scenarios of those loads. Therefore, a new technology based on the concept of creating an electrical network inside conventional concrete has been used to enable its employment in these many applications, including early detection of damage before its development through the concept of electrical resistivity of the network formed inside the matrix by functional fillers prepared for this purpose [1-9]. The transition from traditional concrete to advanced smart concrete requires materials that integrate with the structure of regular concrete and develop it. The most important of these materials are carbon fillers of different types, whether macro, micro, or nano. Among these different types, nanocarbon materials have received wide-ranging attention, focusing on studying the effect of these fillers on the behavior of cement compounds, which can be produced in many important applications such as self-sensing of damage before it worsens, which can achieve low cost and eliminate the disadvantages of integrating electronic sensors in terms of sensing, durability, or

incompatibility with cement structures [4, 10-16]. Previous investigations have shown that some nanomaterials, called zero-dimensional, did not prevent the development of cracks [17, 18]. Graphene nanoplatelets (GNP) are a type of carbon nano-fillers that has caught the attention of researchers working in the field of Engineered Cementitious Composites (ECC). They have shown a unique ability to improve the durability and strength of concrete structures to various kinds of stresses. They have also been shown to create an electrically conductive network inside the cementitious matrix, which can be utilized in a variety of related applications such as thermal and electrical applications. This is attributed to the precision of the graphene nanoplatelet (GNP) particles, which distinguish them by their regular distribution and lack of clump formation within the matrix [19]. Even at low dosages, graphene nanoplatelet composites demonstrated excellent behavior in terms of electrical conductivity and conductive network structure within innovative cementitious composites. Although the small dosage affects the recording of electrical resistivity data, it still results in a remarkable improvement in the mechanical properties of the matrix and the piezoresistivity properties [20-22]. Drawing from the previously reviewed literature and aiming to address a knowledge gap in this field, this paper conducts a study on the impact of GNP on the behavior of the cement matrix. The filler's weakness in bridging cracks prompted the reinforcement of the matrix with two types of fibers: polyvinyl alcohol (PVA) fibers and nylon fibers (NF). This reinforcement aims to enhance the mechanical behavior [22] and investigate its impact on the matrix's response to self-sensing of damage in a hybrid form with GNP. Four treatment ages were adopted for the samples with potable water at room temperature: 28, 56, 90, and 180 days from the initial treatment, and the samples were subjected to four types of loading conditions: compression, splitting (indirect tension), three-point bending, and direct tension. The electrical data were recorded synchronously with the applied load for every second to know the behavior of the samples to damage under the applied stresses until failure over time.

1. Smart Matrices, Materials

It is crucial to understand the fundamental materials and functional fillers that work together to form the self-damage-sensing of ECC. The materials utilized in the production of the samples can be categorized into basic materials, conductive fillers, as well as reinforcing fibers. In this study, graphene nanoplatelets (GNP) with a surface area of 30–60 m^2/g, and a maximum density of 0.03-0.1 g/cm^3, and purity greater than 95% was used as a conductive additive for self-sensing (Figure 1-a). The GNP dosage was maintained at 2% by weight of the cementitious materials during the study. To enhance the matrix strength, two types of reinforcing fibers were employed. The first fiber was polyvinyl alcohol (PVA) measuring 8 mm in length and 39 µm in width. The fibers exhibit a modulus of elasticity of 42.8 GPa, a tensile strength of 1620 MPa, and a specific gravity of 1.3 (Figure 1-b). The second type of reinforcing fiber was nylon fiber (NF), measuring 19 mm in length and 0.55 mm in width with a tensile strength of 966 MPa, an elongation of 35.2%, and a moisture content of 14.46% (Figure 1-c). Ordinary Portland cement (OPC) type I was utilized as the raw material, adhering to Iraqi Standard Specification No. 5/1984 [23] and (Figure 1-d). Silica sand serves as a fine aggregate in mortar formulations. The largest particles measured 0.4 mm, with an absorption capacity of 0.3% of their weight and a specific gravity of 2.6 (Figure 2-e). Class F fly ash (FA) was utilized, adhering to ASTM C 618 [24] (Figure 1-f). The entire mixtures utilized potable water. ViscoCrete® 5930 superplasticizer was utilized for workability, conforming to ASTM-C494/C494M [25] Type F with a specific gravity of 1.095 kg/L. Table 1 presents the chemical and physical properties of PC, FA, and silica sand.

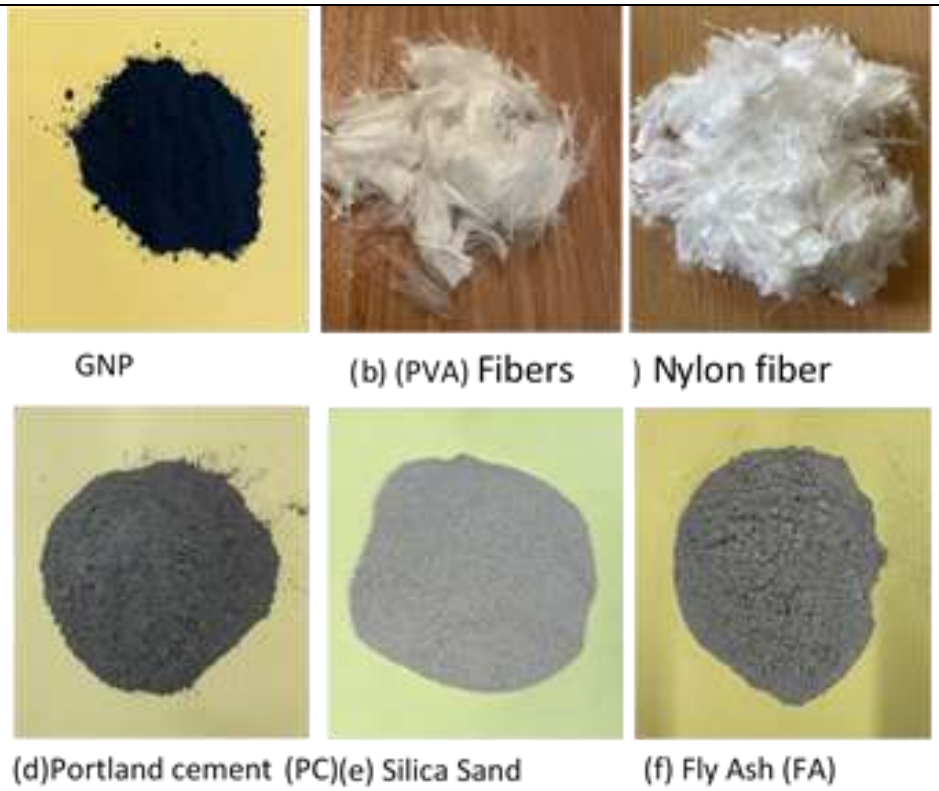

Figure 1: Examples of materials utilized in the manufacture of smart mixtures

Table 1. Chemical properties and physical characteristics of opc, fa, and silica sand

Chemical composition, %	OPC (wt.%)	FA (wt.%)	Silica sand
CaO	63.35	8.08	--
SiO_2	21.65	51.98	>= 50 - <= 100 %
Al_2O_3	3.52	17.04	--
Fe_2O_3	4.87	6.55	--
MgO	3.79	2.14	--
SO_3	2.03	0.025	--
Loss on ignition (LOI)	2.05	10.33	--
Insoluble residue	0.71	-	-
Lime saturated Factor	0.89	-	-
Physical properties			
Specific gravity	3.16	2.09	2.65
Blaine fineness (cm2 g−1)	3941	2689	----

Previous research [3, 26-30] indicated that the percentage (FA/OPC) was 1.2, whereas the ratio of water to cementitious materials (W/CM) was 0.27. To achieve an optimal working ratio, two distinct superplasticizer concentrations were applied based on the kind of reinforcing fibers utilized each time. In mixes reinforced with PVA, 3% by weight of the cementitious components was used, while 1% was the recommended amount for combinations reinforced with nylon fibers. The amounts used for the additions of GNP, PVA, and NF were 2% by volume [31]. The basic elements were combined in a 20-liter Hobart mortar mixer at 100 rpm for 10 minutes. Subsequently, the pre-prepared solution of

superplasticizer and GNP nanofiller was gradually introduced to the dry mixture while maintaining the mixer at a speed of 100 rpm for 10 seconds. The wet and dry mixes were then combined for an additional 10 minutes at a mixing speed of 300 rpm. After that, the mixer was reduced to 100 rpm to add the reinforcing fibers, followed by a return to 300 rpm for an additional 10 minutes to amalgamate the entire components [31-33].

2. Mechanical Tests

This section presents the types of loads applied to the specimens, including compressive strength tests, splitting strength tests, three-point flexural strength tests, and finally direct tensile testing. As mentioned in the introduction section, we applied this procedure for four curing ages. This approach aims to achieve more accurate and realistic results that reflect the self-sensing operation under various loading conditions.

A. Compression test

The compression examination was conducted beneath stress control utilizing a digital electrical testing machine (ELE) with a capacity of 2000 kN and a loading rate of 0.9 kN/sec. The test was conducted beneath constant load until failure on three samples from every set being examined as shown in Figure 3-a. A cubic mold with dimensions of 2 inches (50 mm) was utilized for pouring the blend, and compression evaluation was conducted following the procedures outlined in [34].

B. Indirect tensile test

The test was conducted following the guidelines outlined in [35], employing an (ELE) ADR Touch SOLO 2000 BS EN Compression Machine equipped with a digital readout and self-centering platens that operates at a loading rate of 0.9 kN/sec, utilizing 50*50*50 mm cubic specimens positioned among two square bars measuring (width 10× height 10) mm as shown in Figure 3-b. All specimens of the mixture underwent testing for splitting tensile strength until failure, with consideration given to their average values.

C. Bending strength test

The bending test was conducted on prismatic specimens with dimensions of 40 mm × 40 mm × 160 mm, according to [36]. The smart prisms were mechanically evaluated by supporting them at two points separated by a distance of 120 mm, which corresponds to the exact distance between the two poles placed inside the prism. Then, the load was applied using a 200 kN digital testing machine (WDW-200E) connected to a computer data logger; the applied load rate was 0.5 mm/s. The software in the testing machine documented the correlation between the bending force, deflection, and time. Figure 3-c shows a picture of the specimen inside the machine.

D. Direct tensile strength test

The direct tension method was used to perform the direct tensile strength test, as mentioned in [37]. A 10 kN ELE mechanical testing equipment was used at a load rate of 0.02 kN/s on dog bone specimens, measuring 40*75*25 mm, and three specimens of each combination design at intervals of 28, 56, 90, and 180 days when testing. Figure 3-d shows the specimen inside the apparatus during testing.

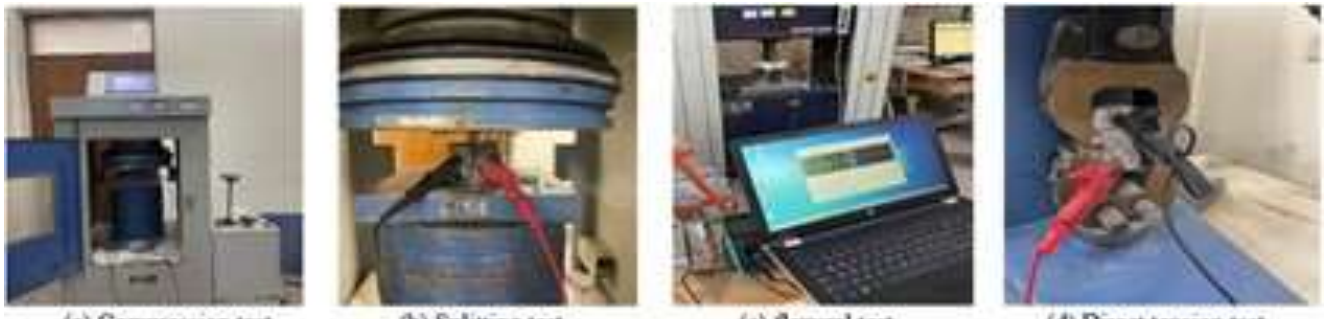

Figure 2: Mechanical test setups

E. Investigation of electrical resistivity

To assess the self-sensing ability, smart ECC composites using carbon-based conductive elements were produced. The sensing behavior of smart specimens composed of graphene nanoplatelets (GNP) reinforced with PVA and nylon fibers under four loading conditions: monotonic compressive load, indirect tension load, three-point flexural load, and direct tension load was examined. The self-sensing performance was assessed for each matrix in terms of detecting the fractional change in electrical resistance (FCER) in response to the applied load type. The proposed configuration for this study entails utilizing 50 mm cube samples for compressive and splitting stresses, while prismatic specimens with dimensions of 40 mm × 40 mm × 160 mm and dog bone specimens measuring 40 mm × 75 mm × 25 mm were used for flexural and direct tension tests, respectively. To avert the polarization effect caused by curing the materials in water, the samples were oven-dried at 60 °C for a full day before testing at all specified research ages (28, 56, 90, 180 days). To evaluate the damage-sensing capability of the fabricated samples, electrodes were embedded into them when they were fresh, utilizing strips of brass plate measuring 75, 60, and 40 mm in length for cubic, prismatic, and dog bone samples, respectively with 10 mm in width and 0.1 mm in thickness. The resistance of these strips is 0.3 ohms, and they were symmetrically positioned around the center of the sample, as illustrated in Figure 4. This arrangement is consistent with previous studies [2, 3, 26-28, 38, 39]. The electrical resistance was measured using the Pro'sKit MT-1820 DC Multimeter [40]. The interaction between the sample and the loading test apparatus was accounted for; thus, wooden strips were positioned above and below the sample to mitigate the interference with the electrical signal transmitted to the electrical resistance tester by the mechanical testing machine. The electrical resistance and mechanical strength measurements were recorded simultaneously for each second under identical loading conditions. This indicated that the mean mechanical resistance values and the relative variation in electrical resistance (Equation 1) may be graphed as a function of time.

$$FCER\left[{}^{\Delta R}/_{RO}\right]\% = \left(\left[\!\left[RL - RO\right]\!\right] / RO\right) \times 100$$

where RO stands for initial electrical resistance, FCER for fractional changes in electrical resistance, and RL for electrical resistance under loading at a specific time during the test.

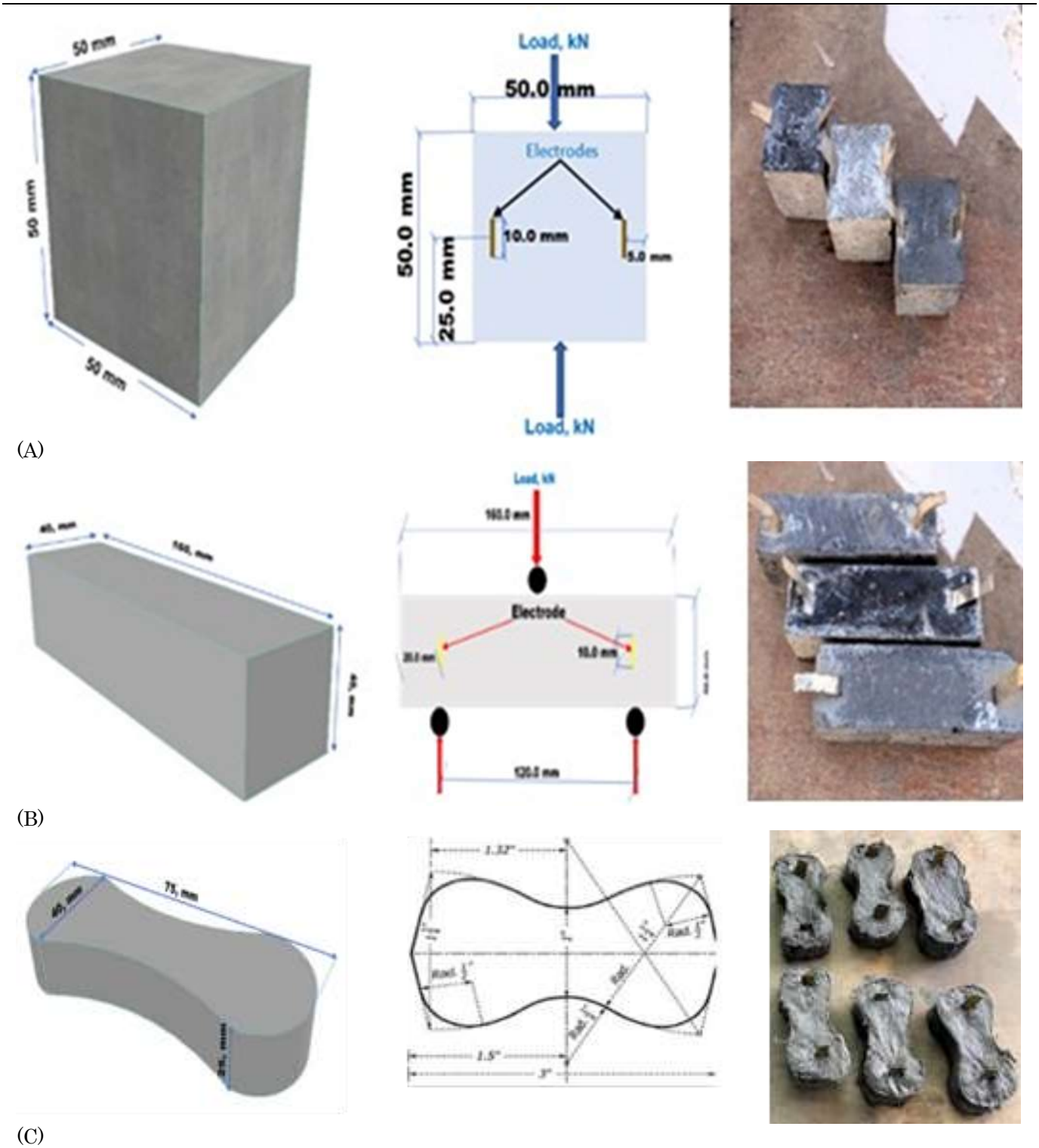

Figure 3: The geometric dimensions of the various specimens: (A) cubic, (B) prismatic, and (C) dog bone.

3. Results And Discussion

This section displays and evaluates the test outcomes for mortar samples with and without conductive components during curing durations of 28, 56, 90, and 180 days. The study looked at how well self-monitoring worked in new mortar mixes that had

nano-scale conductive fillers and different kinds of strengthening fibers added to them. It concentrated on mechanical qualities, such as splitting tensile strength and compressive strength. Prior to analyzing and assessing the outcomes of self-damage detection in mixtures composed of smart electrically conductive nano-fillers augmented with mechanical reinforcement fibers in this study, it is imperative to evaluate the impact of these fillers on strength and durability characteristics, particularly in comparison to control mixtures (lacking functional fillers and reinforcement fibers), which will be more pronounced at the study intervals of 28, 56, 90, and 180 days. Figure 5 shows the average compressive strength values of 2-inch cubic specimens. The innovative blends show excellent performance under uniaxial compressive strength for both the smart blends (GNP-PVA, GNP-NF), as well as for all the proposed ages covered in this study. When the specimens were aged, their compressive strength increased steadily over time. This showed that the NF-reinforced blends were stronger than the PVA-reinforced blends. The improvement of GNP-PVA blends between 28-180 days was 31%, while when compared to the conventional blends, the strength development percentages for ages 28, 56, 90, and 180 were 48%, 48%, 52%, and 24%, respectively. The gradual improvement of the GNP-NF mixture between 28-180 days was 25%, while the percentage compared to the normal mixtures for ages 28, 56, 90, and 180 days was 55%, 60%, 52%, and 24%, respectively. The results presented in Figure 5 align perfectly with Dong, et al. [8] findings about the beneficial impact of GNP on enhancing mechanical behavior under uniaxial compressive stresses at a concentration of 2% by weight of the mixture, even though the compressive strength values in this work clearly increase with age. Over time, the C-S-H gel hardens, creating a continuous binding matrix with a large surface area that is the main part of the cement paste that makes it stronger [41]. This is because GNP has a very large surface area, which acts as a clear stimulus for the hydration process and makes it easier for the gel to stick to the surface of cementitious compounds. The nanoplatelets also help the crystallization process, which bridges the cementitious matrix. The incorporation of PVA fiber into the cementitious composites enhances the durability of the cementitious compound, particularly in relation to cracking, which is influenced by the connection qualities at the interface of the fiber-matrix [28, 42, 43]. Regarding the nylon fiber-reinforced GNP matrix, the fibers have a significant role in improving the strength of the mortar under compressive load. The mechanism of distributing the applied load at the fiber-matrix interface is responsible for this improvement. The flexibility of the reinforcing fibers embedded in the matrix increases the flexibility of the matrix, which makes the fibers flow under the applied load without breaking, especially when the length and concentration of the fibers in the matrix are high [44, 45]. Figure 5 demonstrates the superiority of GNP-NF mixtures over GNP-PVA mixtures, particularly at early ages, with all mixtures demonstrating the same level of strength at late ages. The reason for this could be attributed to the ongoing hydration and gel formation processes, which enhance the bonding strength between the cement interface and the reinforcing fibers, particularly the nylon fibers [41].

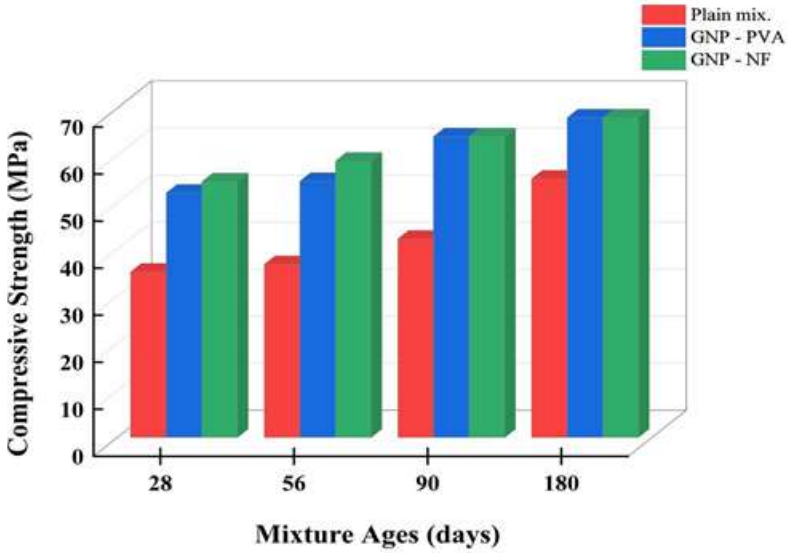

Figure 4: Results for compressive strength for various innovative blends ages group

The average indirect tensile strength values of three 2-inch specimens of each type of mix for both early and late curing ages are shown in Figure 6, comparing the new smart mixes of nanofillers injected with graphene nanoplatelets and reinforced with reinforcing fibers to the reference matrices for the aforementioned study ages. When evaluating the capacity of the mixtures under this type of loading, Figure 6 reveals a significant improvement in the indirect tensile strength values for the late ages. There was a clear drop in the indirect tensile strength values at early ages. However, this behavior is very similar to how the samples behaved when they were subject to the compression load, which supports what scientists think (Section 3.1.1) about how fillers behave in the cementitious system. The superiority of the mixes reinforced with PVA fibers was recorded over those reinforced with nylon fibers, indicating that the nanofillers and the reinforcing fibers of the regular matrix had a clear positive synergistic effect on the development of the split tensile strength. The development ratios of the smart mixes compared to the control mixes can be summarized as follows. For example, the gradual improvement with curing age of the GNP-PVA matrix at 28, 56, 90, and 180 days was: -22%, 21%, 68%, and 68%, respectively. At 28, 56, 90, and 180 days, the GNP-NF matrix developed strength values of -33%, 21%, 55%, and 65%, respectively. The strength development from 28 to 180 days of the GNP-PVA blend was 195% from 2.1 to 6.2 MPa, while that of the GNP-NF blend was 239% from 1.8 to 6.1 MPa. The presence of carbon-based nano-sized fillers interacts with PVA fibers through their absorption by the fibers, resulting in high frictional bonding strength and improved ductility properties during the formation of primary cracks under cleavage tensile stress. This interaction explains the improvement in cleavage tensile strength values of smart blends, particularly with GNP-PVA blends [46]. Bheel, et al. [47] attributed the improvement in the tensile strength properties of the split to the synergistic effect of nano-graphene with PVA fibers, which improves the ductility of the matrix and the stiffness upon stress, as well as enhancing the area under the strain-hardening curve. The probe settings applied to the specimens tested in this paper may enhance the mechanical behavior of this type of stress which confines the load to the region of indirect tensile stress distribution [31]. The results presented in Figure 6 for the GNP-NF matrix are in complete agreement with the findings of Ahmad, et al. [48], who demonstrated that nylon fibers significantly enhance the cement matrix's resistance to indirect tensile strength, particularly at the age of 90 days from the initial curing. This is in line with the results of this work, which show the development of strength at later ages. This improvement is attributed to the bonding strength between the fibers and the cement paste. Despite the limited experimental procedures in this paper for this type of load and the fillers incorporated in the cementitious system, the behavior of late ages develops due to the nano additives' ability to delay hydration reactions. This interaction provides

continuity to the hydration components, thereby enhancing the mechanical properties of late ages. So, more splitting tensile tests need to be done to find out more general scientific facts that can explain how nanofillers (GNP) act by themselves or in hybrids.

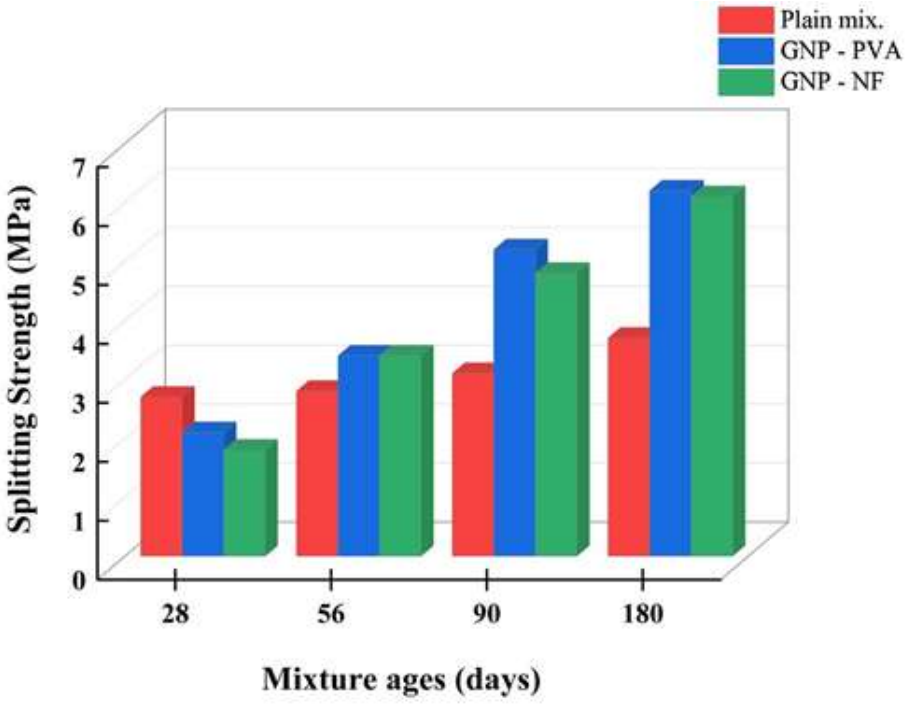

Figure 5: Indirect tensile strength of intelligent mixtures in relation to age

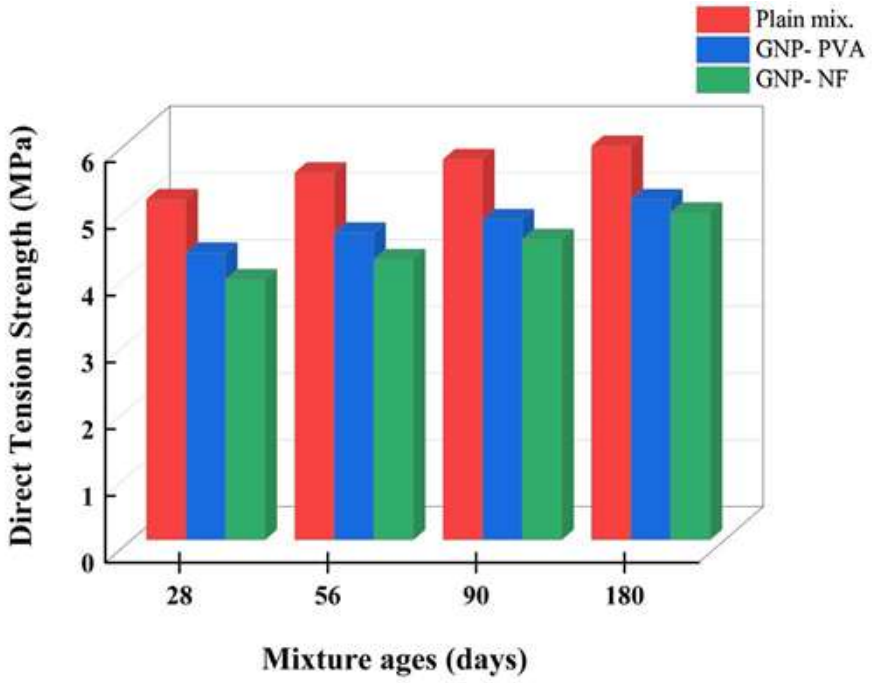

Figure 6: Direct tensile strength of different mixtures in relation to age

Figure 7 shows the average direct tensile strength values of three 75×40×25 mm dog bone specimens of each type of mixture over the study ages. This study compares the innovative nanofiller and fiber-reinforced smart mixtures with the reference mixtures of the same ages to determine the effectiveness of the fillers incorporated into the plain matrix under this type of loading, as well as the extent of improvement or lack thereof in the mechanical properties. The direct tensile strength of all mixtures and all treatment ages was clearly lower than that of the reference mixtures, even though they all had the same amount of mechanical reinforcement fibers added to them. The behavior was consistent, showing a decrease in the tensile strength of the smart matrices compared to the control mixtures and a gradual increase in tensile strength as the matrices aged. This decrease aligns with the findings of Lv, et al. [49], who demonstrated that the direct tensile strength starts to decline at a concentration of GNP greater than 0.03% of the cementitious weight, and that the decrease in tensile strength increases with the dosage. This is due to the regular crystallization of GNP at this dosage, which increases the density and reduces the pores within the cementitious system. However, increasing the dosage of GNP beyond 0.03% leads to irregular agglomeration, also known as irregular polyhedral, which the matrix can benefit from in compressive strength loads. This behavior is fully supported by the behavior of the matrices in this paper at a dosage of 2% by weight of cementitious composites in both compression and direct tension. The innovative matrices recorded a decrease in tensile strength compared to the reference mixtures, but their behavior was consistent in terms of strength development with age and the superiority of PVA-reinforced matrices over those reinforced with nylon fibers as previously mentioned in Section 3.1.2. One reason the GNP-PVA matrix is better than other fibers that PVA fibers have unique physical properties [50, 51]. In addition, the synergistic effect of PVA fibers along with GNP increases the strength of the area under load [47]. This is consistent with what was concluded by [33] that fibers in general and PVA in particular have a bridging phenomenon that prevents the transmission of cracks through the matrix and their exacerbation, which develops the resistance of the cement matrix to the following tensile forces [52]. The strength development of smart blends from 28 to 180 days can be summarized as follows. For example, the strength development of the GNP-PVA blend from 28 to 180 days of initial curing was 19%—from 4.3 to 5.1 MPa, while the strength development of the GNP-NF blend from 28 to 180 days was 26%—from 3.9 to 4.9 MPa.

Before looking at the results of self-damage sensing, it is important to see how these additives changed the durability properties at 28, 56, 90, and 180 study ages compared to the control mixtures in this study. Figure 8-a displays the average flexural strength values, while Figure 8-b displays the average flexural deflection for three prismatic samples measuring 40×40×160 mm. By comparing the findings to the reference arrays, a clearer picture may be obtained. Figure 8 displays that the flexural strength of the new combinations got stronger over time. This indicates that the GNP-PVA and GNP-NF smart mixtures function effectively under load and for all the suggested ages in the research. Based on the findings, mixes reinforced with NF fibers were better than those reinforced with PVA fibers. Compared to the plain mixes, the functional mixture GNP-PVA showed an improvement percentage of 107% at age 28, 142% at age 56, 68% at age 90, and 53% at age 180. The GNP-NF combination showed a 117% improvement at age 28, a 139% improvement at age 56, a 109% improvement at age 90, and a 95% improvement at age 180. In general, the results presented in Figure 8-a clearly show the improvement in the average flexural strength of the innovative matrices with age and are superior to the reference mixtures for the same proposed curing age. These results are in complete agreement with what was reached by Yıldırım, et al. [31], who attributed this improvement to the increase in the amounts of superplasticizer used in mixtures containing PVA fibers, which leads to delaying the development of the properties of the fibers and the cement matrix interface, which in turn directly affects the development of the flexural strength [53, 54]. The improvement in smart matrices and their superiority over reference mixtures is due to their incorporation

of additives, whether conductive or strength-enhancing. For example, GNP plays an important role in developing flexural strength by accelerating and continuing the wetting processes even at late ages [55]. The decreased flexural capacity at late ages with regular behavior for both GNP-PVA and GNP-NF matrices while maintaining their superiority over the reference blends may be due to the increased amounts of GNPs, which make it difficult to distribute them homogeneously with the increase of agglomerations within the matrix, which negatively affects the hydration process, density, and pores [56]. The superiority of GNP-NF matrices is due to the behavior of nylon fibers under bending loads resulting from high elongation of nylon fibers in addition to the length of nylon fibers used in this investigation of 19 mm which improves the peak bending value and beyond [57]. Moreover, the late-age hydration processes have improved, and the bonding of fibers with cement paste has strengthened the behavior of nylon fibers [41]. The findings varied with treatment age for the average deformation values under flexural stress; this was true for both the regular and smart mixes. The deformation values of the reference mixes kept going down because of the hydration process and matrix hardening. This made the first crack grow faster. The novel carbon-based matrices exhibited different behavior in the early and late ages, with the latter showing a significant rise in the deformation values. This could potentially be attributed to the interaction between the fibers and the matrix, as well as the GNPs, which act to bridge the fractures, thereby reducing the rate of matrix failure. All the findings from [58] align with this conclusion.

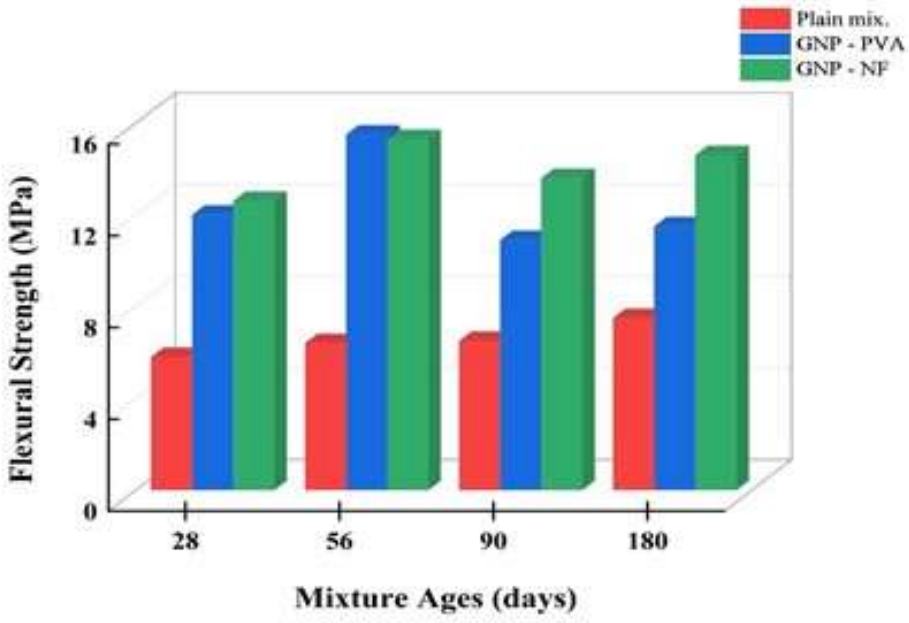

Figure 7: Flexural strength of different mixtures in relation to age

3.1. Self-sensing experiments under uniaxial compressive stress

The impact of carbon-based conductive fillers reinforced with PVA and NF fibers on the sensing capabilities under uniaxial compressive loading circumstances for varying processing ages is discussed in this part, along with the results of laboratory experiments conducted on samples made using these fillers. Figures 9–11 illustrate the self-sensing behavior of the control mixture and the smart mixtures (GNP-PVA and GNP-NF). They display the FCER relationship over time under an applied load. The dashed lines show the fractional change in electrical resistance, whereas the solid

lines show the evolution of applied load values. The self-sensing response behavior of the control mixtures under compressive force at ages 28, 56, 90, and 180 is depicted in Figure 9. The control mixtures function exceptionally well, showing a steady rise in sensing levels under load, beginning at zero, even with the small FCER values and the lack of conductive fillers. In ordinary ECC-plain samples, the conductive phases may split when an electric field is introduced. A piezoresistive response may result from the micropores holding an endless amount of water and dissolved ions [28, 59]. The availability of fly ash class F, which can be thought of as the foundation of smart mixtures that cannot be dispensed with on a mechanical or electrical level, coupled with other functional fillers, definitely increases the likelihood that this response will be possible [60]. Early ages exhibit high FCER values, followed by successive declines for late ages. This is because the process relies on the amount of hydration water present in the initial reactions before starting to diminish as the gel filling the pore forms [30, 31, 61, 62]. Figures 10 and 11 show the structural health monitoring behavior of the innovative and smart cementitious composites under uniaxial compressive loads up to failure. The response of the smart arrays to sensing the damage resulting from the loading is evaluated in comparison with the self-damage-sensing behavior of the control arrays, which is more pronounced, and then the innovative composites are compared with each other depending on the type of reinforcing fibers embedded in them and the effect of each on the self-sensing values of the applied compressive load. Looking at Figures 10 and 11, it can be noted that the innovative matrices GNP-PVA and GNP-NF are superior to the reference mixtures in terms of the development of the sensing values known as ΔR/RO, or the fractional change in electrical resistance. The observation becomes clearer at early ages than at late ages. This behavior is considered normal due to the development of the polarization process at early ages as a result of the abundance of water that has not yet participated in the hydration process, which provides fewer pores and freer ion movement, and the lack of development of gel formation, which is a cause of weakening the conductive network within the matrix at late ages accompanied by a decrease in hydration water. Therefore, see high sensing values at early treatment ages, then they begin to decrease with the progression of treatment age [31, 63, 64]. There are no significant differences in the self-sensing behavior of the GNP-PVA and GNP-NF matrices reinforced with two different types of reinforcing fibers. This might be because of how the graphene nanosheets behaved when they were injected into both matrices at the same concentration. Earlier research has shown that these nanosheets can fill in cracks and make the network better at conducting randomly under load. This lets ions move easily between the electrodes so that the values of the change in resistance under load can be recorded [20, 65]. The observed improvement in sensing behavior in all mixtures that was detectable from the beginning is likely to be due to the optimum concentration of GNPs, which is considered the leakage threshold limit that gives the best sensing behavior under loading. This is in complete agreement with the conclusion of Dong, et al. [8] who confirmed that the optimum leakage threshold for GNPs is between 2-3% by weight and gives the best behavior in increasing the electrical conductivity of the network within the matrix [4].

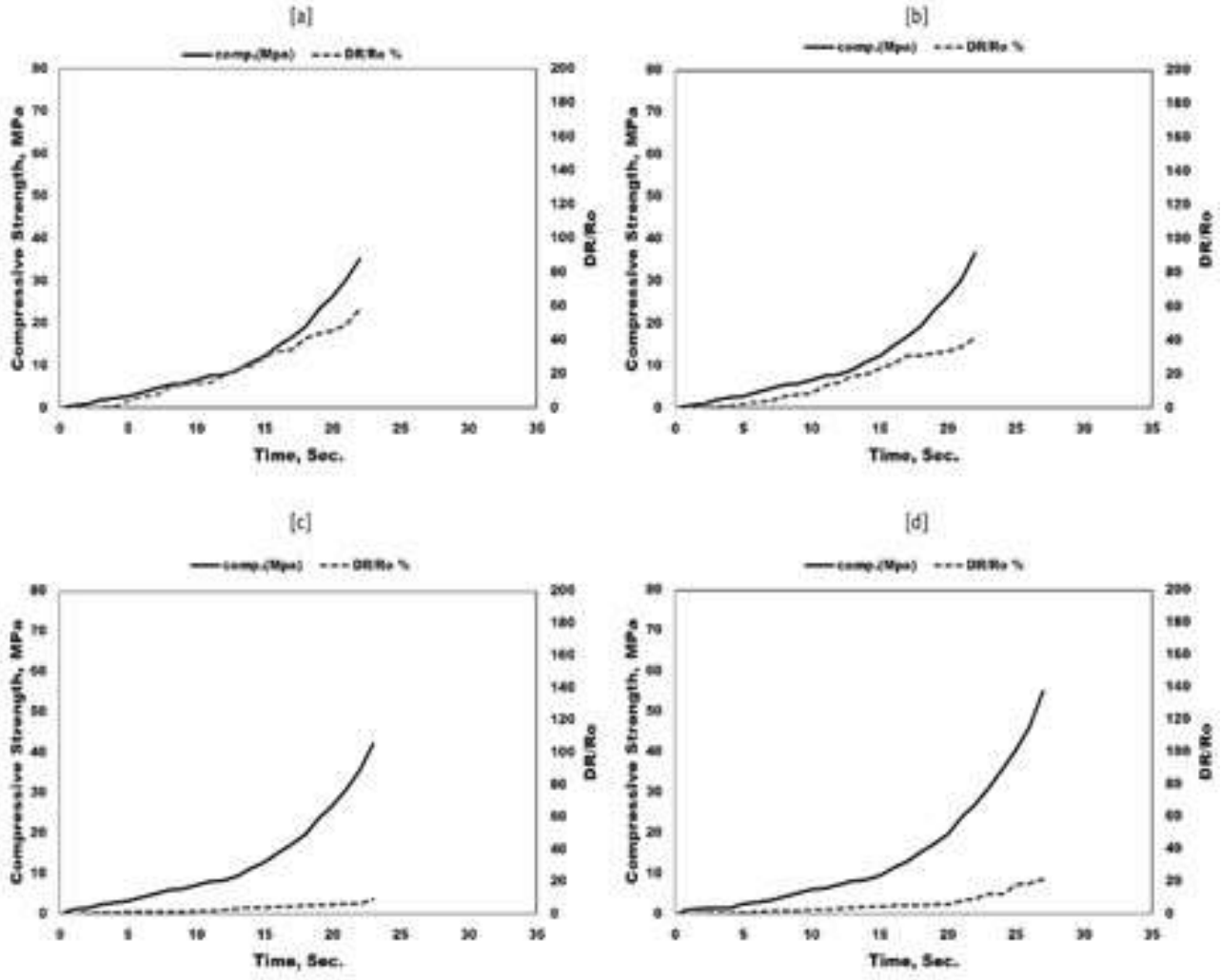

Figure 8: Self-sensing of reference mixtures under uniaxial compressive strength for different curing age; a)28 days, b)56 days, c) 90 days, and d)180 days.

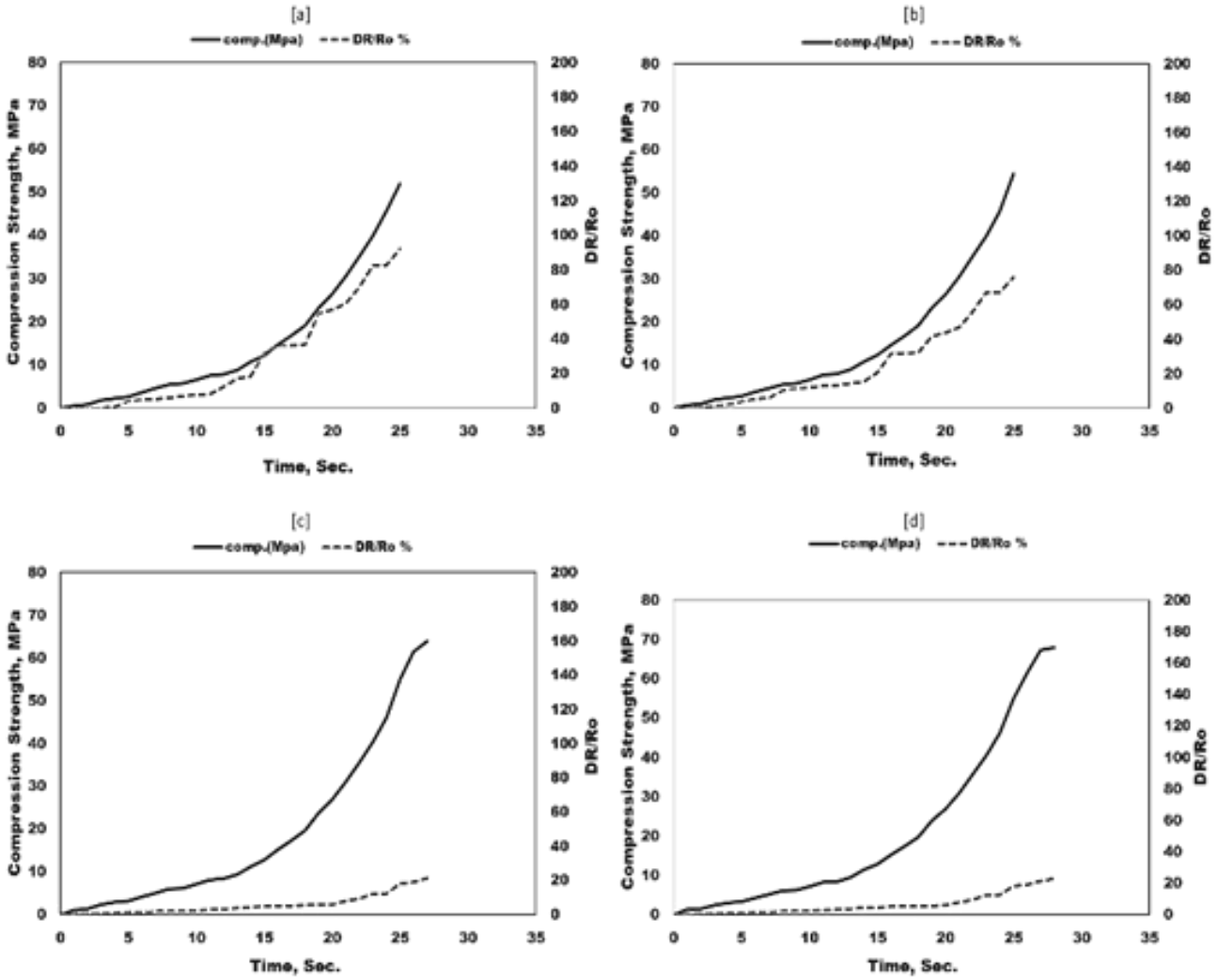

Figure 1: Self-sensing of GNP-PVA mixtures under uniaxial compressive strength for different curing age; a)28 days, b)56 days, c) 90 days, and d)180 days

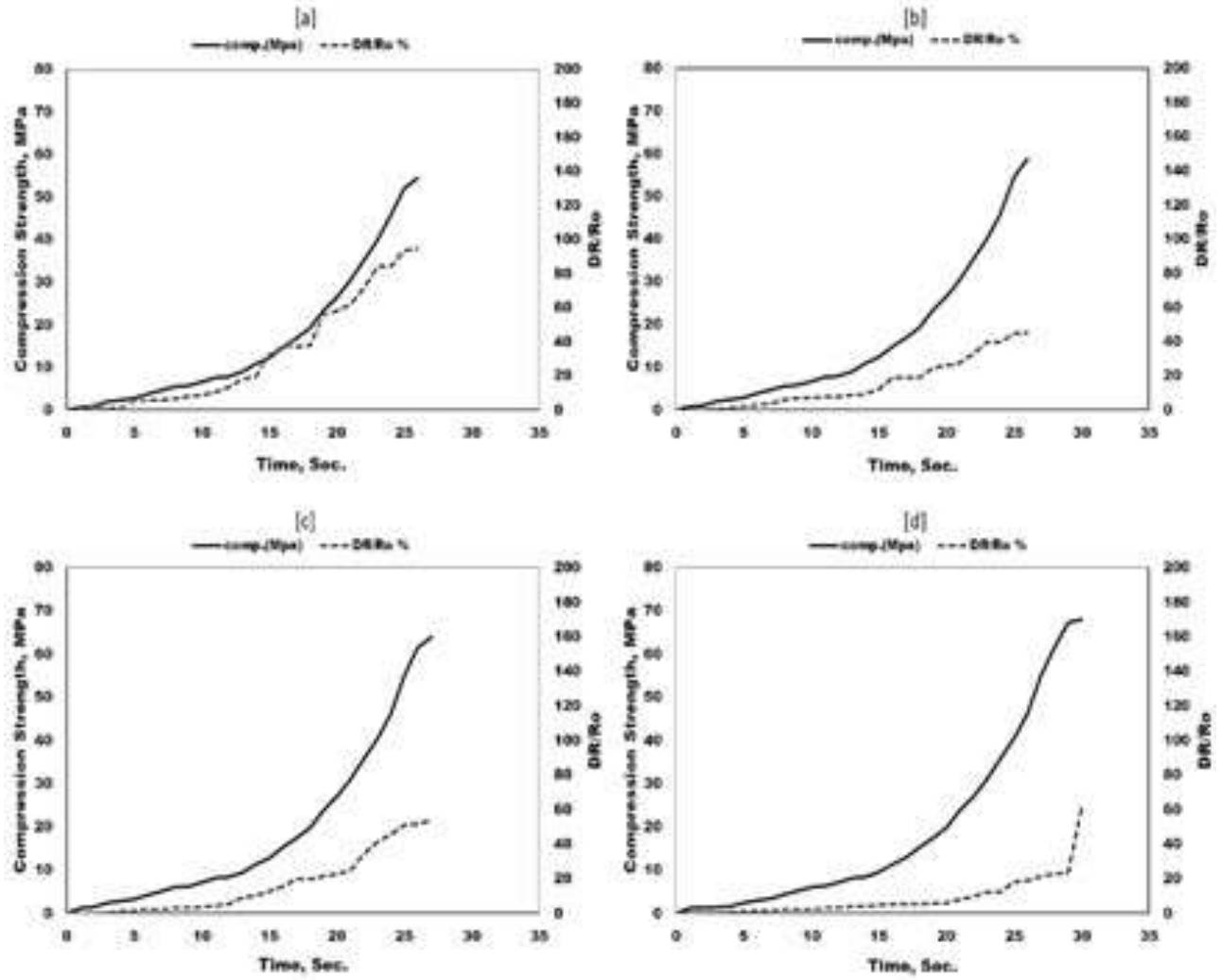

Figure 2: Self-sensing of GNP-NF mixtures under uniaxial compressive strength for different curing age; a)28 days, b)56 days, c) 90 days, and d)180 days

4. Self-sensing performance under indirect tensile stress

The evaluation of the sensing capability of cementitious composites beneath this specific loading condition is crucial. Initial observations indicate the formation of a single microcrack, which subsequently expands and develops into multiple cracks with ongoing loading over time. Ultimately, a single crack emerges, allowing for the recording of self-sensing data. The self-sensing capability of the median of three 2-inch samples is illustrated in Figures 12–14, which underwent indirect tensile stresses corresponding to the ages outlined in the aforementioned study. The electrodes were directly added to the top surface of the specimen, positioned at a distance of 0.5 cm from the edges of the cube specimens, resulting in a confined self-sensing region [31]. The manner in which a sample fractures under the application of indirect tensile stress in the test setup directly influences the efficacy of the new smart blends in self-sensing characteristics. The graphs can be studied using FCER results and the partial change in electrical resistance data of the functional blends in the present investigation. The performance of the unmodified blends, as shown in Figure 13, was significantly limited, especially at advanced curing ages of more than 28 days. This was demonstrated in Section 3.2.1 regarding the development of sensing at early stages compared to late ages. However, sensing data were not recorded from the beginning until after the damage development stage close to failure. FCER values of the blends made of GNP functional fillers in Figures 13 and 14 showed self-sensing values that were clear and easy to record from the beginning of

the load application compared to the control blends, with a difference in the sensing values between the GNP-PVA and GNP-NF blends; these values were higher in the blends reinforced with PVA fibers compared to the GNP-NF matrix. Looking at Figure 13, the behavior of ages 28 and 56 (Figures 13-a, b) was somewhat similar with modest FCER values compared to ages 90 and 180 (Figures 13-c, d). The development in the sensing values was very clear, reflecting the understandable picture of the development at later ages, and this may be due to the behavior of GNP in continuing the wetting process at later ages and its coating of the PVA fibers and the type of such loading, which makes the sensing ability good at later ages. On the other hand, in Figure 14, the same behavior is seen as that of the GNP-PVA matrix in Figures (14-b, c, d), but with more modest values in terms of the development of the matrix response to sensing at later ages. Microcracks that developed beneath indirect tension load exhibited a more quick and extensive opening compared to those created beneath compression. This difference in behavior was believed to account for the variations observed in the self-sensing characteristics across different matrices. The incorporation of nanofillers within the matrix has notably enhanced the sensitivity of matrices subjected to indirect tensile loads. This leads to the displacement of graphene nanoplatelet molecules, resulting in their separation as microcracks form during loading, which in turn elevates the electrical resistance values [50, 66, 67].

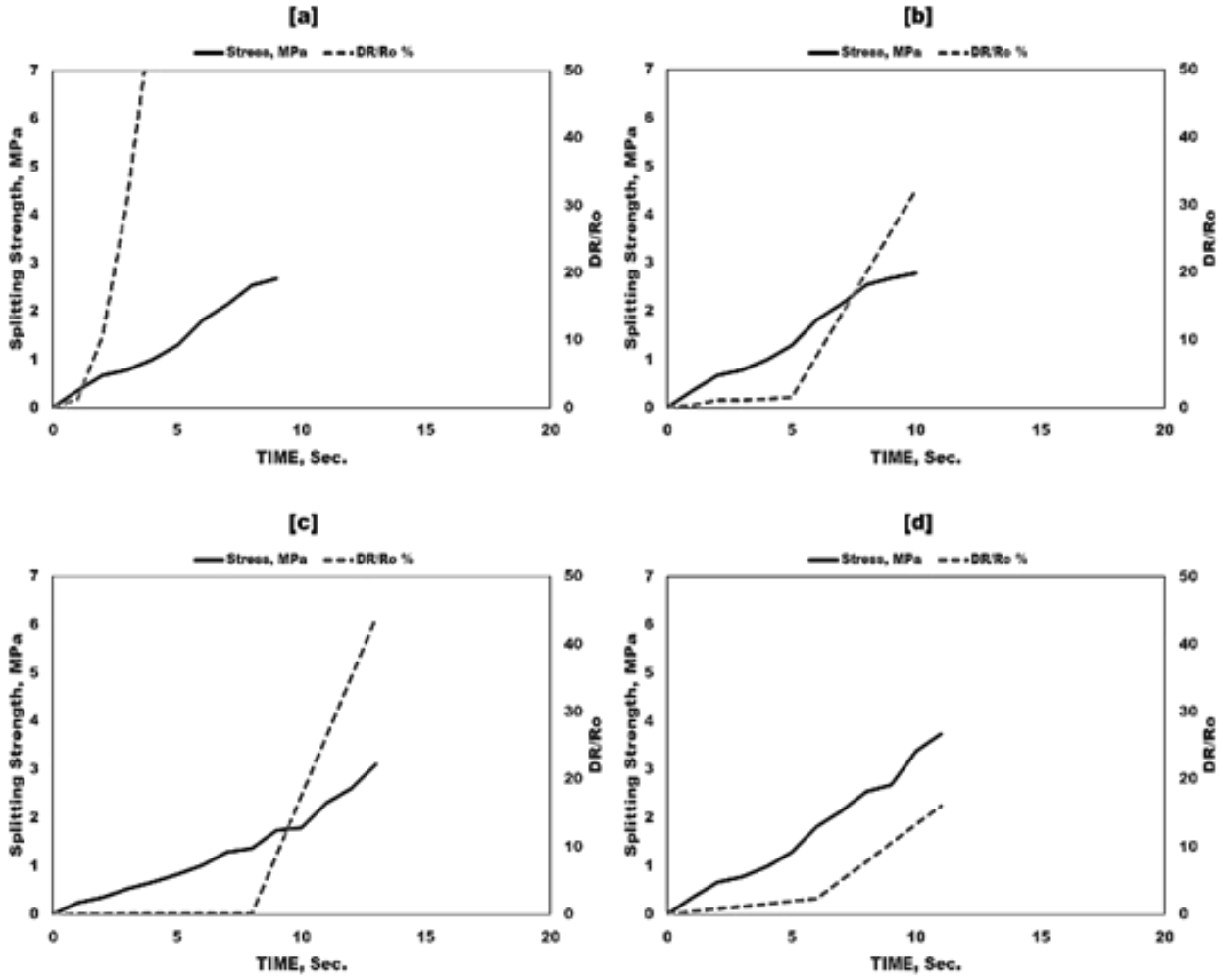

Figure 3: Self-Sensing of reference mixtures under Indirect Tensile Strength for different curing age; a)28 days, b)56 days, c) 90 days, and d)180 days

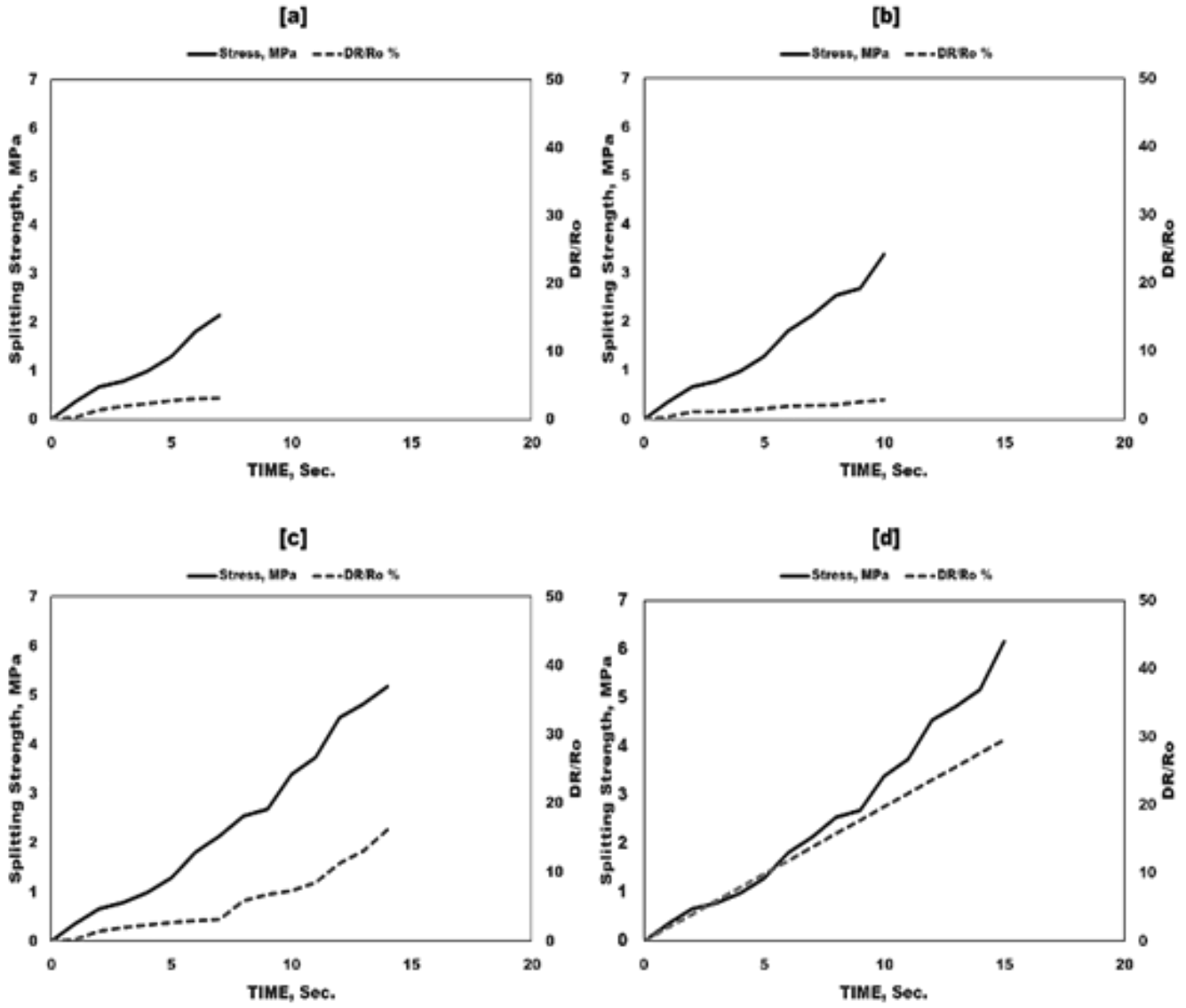

Figure 12: Self-Sensing of GNP-PVA mixtures under Indirect Tensile Strength for different curing age; a)28 days, b)56 days, c) 90 days, and d)180 days

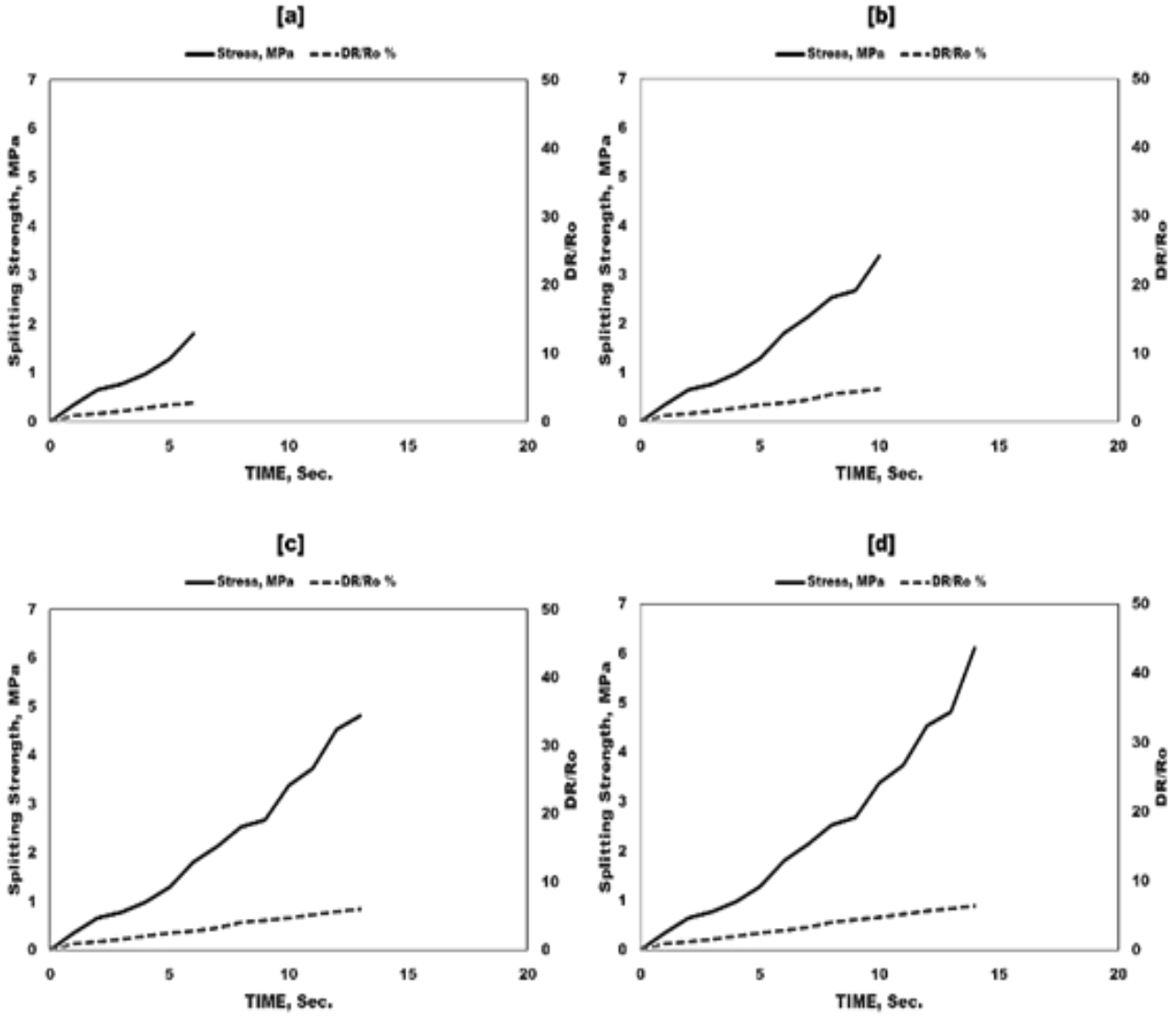

Figure 4: Self-Sensing of GNP-NF mixtures under Indirect Tensile Strength for different curing age; a)28 days, b)56 days, c) 90 days, and d)180 days

5. Self-sensing performance under three-point bending stress

This section analyses and assesses the self-sensing outcomes derived from applying three-point flexural loads to novel samples composed of GNP reinforced with PVA and NF fibers at both early and late curing ages. Figures 15–17 illustrate the self-sensing characteristics of both intelligent and conventional blends. They show how the fractional change in electrical resistance (FCER) is related to both flexural stress (vertical axis) and deformation (horizontal axis). It can record the variations in electrical resistance of all mixes, regardless of the presence of conductive components, from the beginning. This behavior develops permanently in a linear manner, with the FCER fluctuating depending on the matrix type and the curing age for a particular graph. Figure 15 shows how well the control mixes worked for the self-sensing response to bending stress at 28, 56, 90, and 180 days old. Even though the FCER values aren't very high and there aren't any conductive fillers in the control mixes, they work very well, with sensing values consistently going up with load from zero. Some carbon-based materials and electrically conductive phases may be adding to

the samples that are being flexural loaded, which could explain the small changes seen in the FCER results during the elastic phase (the start of the loading), when no cracks can be seen. The sensing values of the reference and clever combinations at early ages may be associated with polarization, attributed to a significant amount of hydration water that has not yet engaged in the hydration reactions. Additionally, the potential existence of micro-cracks within the microstructure of the matrix-aggregate interface may also play a role [31, 62]. The remarkable improvement in the sensing capability of the delayed ages of the smart blends can be attributed to the behavior of GNPs, which delay and continue the hydration processes, thereby providing good conductivity to the formed network. See Section 3.1 for more details. As mentioned in the opening of this section, FCER values showed an irreversible linear growth of the matrix, regardless of matrix type or age. This behavior, prevalent in prismatic samples subjected to flexural stress, is likely attributed to the presence of microcracks in the structure of the mixtures between the interface of the cement paste and fine aggregate or between the interface of the matrix and additives that develop with the application of flexural load over time, leading to the damage of the conductive paths within the electrical network after crack formation due to the gradual flexural load over time. Figures 16 and 18 show the performance of the smart blends GNP-PVA and GNP-NF, respectively, which showed very good behavior compared to the control blends through the significant increase in FCER values. The enhancement of the electrical network within the cementitious system is unambiguously attributed to the injection of carbon dosage at the nanoscale, along with another beneficial effect of raising the sensing values related to the bridging of the fibers across the crack before failure, thus maintaining the network connection with the remaining functional conductive paths [68].

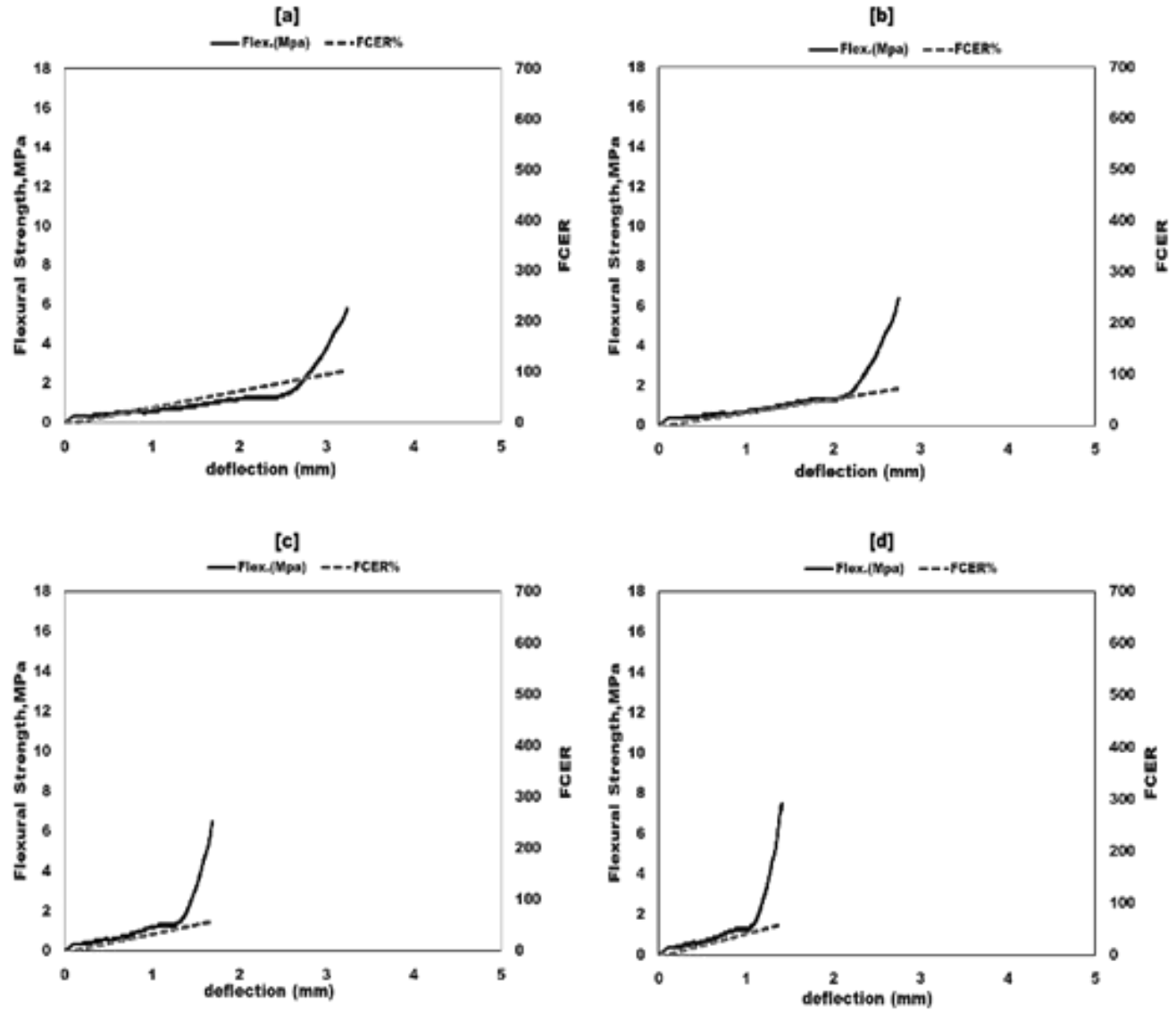

Figure 14: Self-Sensing of reference mixtures under Flexural Strength for different curing age; a)28 days, b)56 days, c) 90 days, and d)180 days

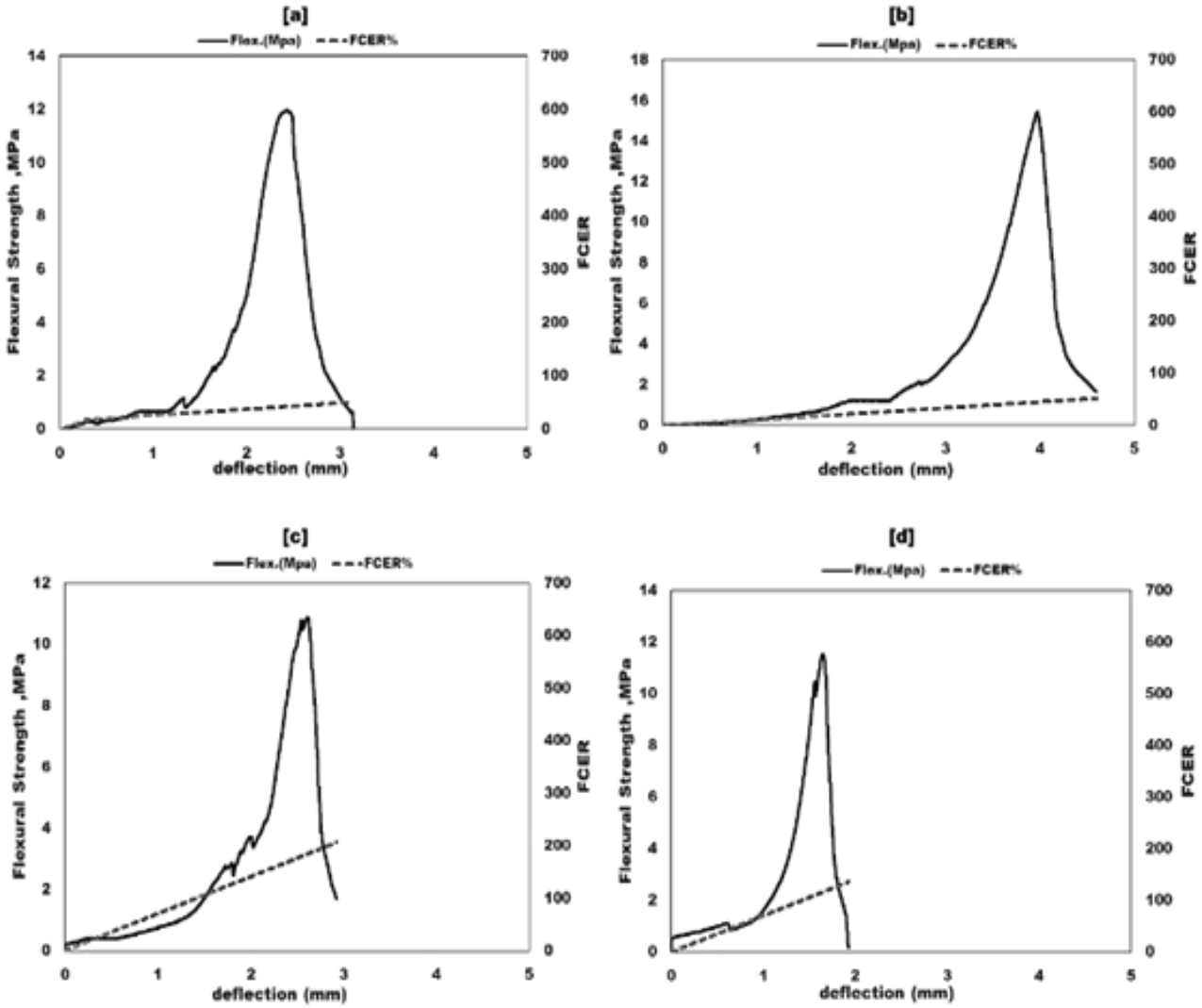

Figure 5: Self-Sensing of GNP-PVA mixtures under Flexural Strength for different curing age; a)28 days, b)56 days, c) 90 days, and d)180 days

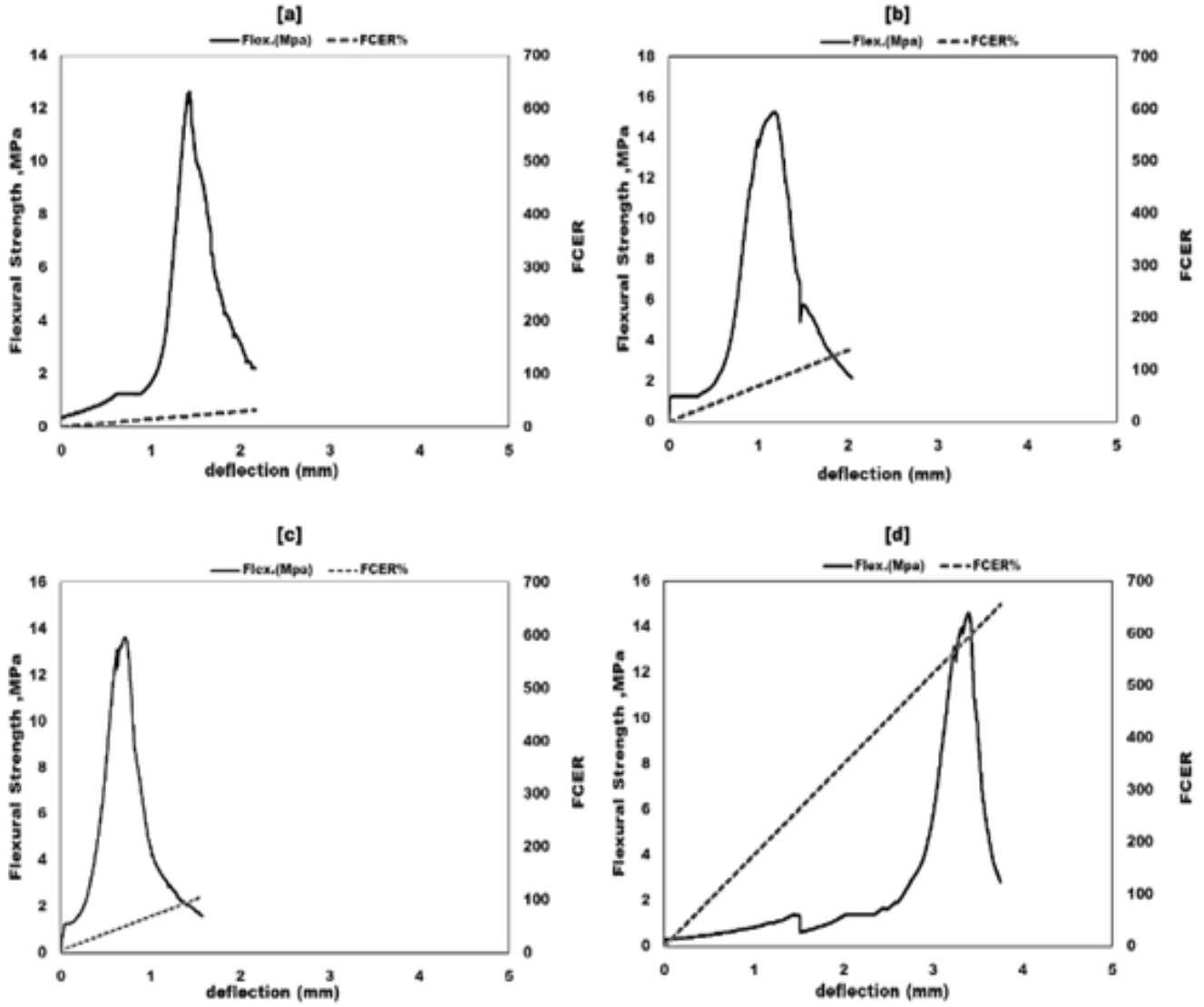

Figure 6: Self-Sensing of GNP-NF mixtures under Flexural Strength for different curing age; a)28 days, b)56 days, c) 90 days, and d)180 days

6. Self-sensing performance under direct tensile stress

Figures 18-20 present a visualization of the behavior of ECC arrays for average damage sensing values under direct tensile loads for the reference and novel clever matrices over time. The remarkable improvement in the self-sensing properties of the matrices developed with conductive nanofillers is due to the activation of electron transfer through tunnelling between nanofillers or fibers-to-fibers [50, 51]. A previous study [44] confirmed that the high self-sensing values under direct tensile forces might be because the fibers embedded in the matrix tend to separate or break when stress is applied. This is similar to how the new matrices in this study that were reinforced with PVA fibers (Figure 19) and nylon fibers (NF) (Figure 20) behaved. The cracking pattern of the laboratory-tested samples may contribute to the differences in the sensing behavior of the smart matrices associated with ages, as it directly influences the matrix's ability to alter its electrical resistance over time until failure [69, 70]. The synergistic effect between the graphene nanosheets (which accelerate and delay the hydration reactions for the late ages), as mentioned

previously, and the mechanical reinforcement fibers covered with nano-fillers, which in turn leads to the contact of GNP molecules with the surfaces of those fibers [71], which makes them a network with well-conductive paths for the late ages. The differences in the self-sensing values of GNP-PVA and GNP-NF blends can be clearly seen; in terms of more regular behavior, GNP-PVA blends developed gradually with the ages of the study. While GNP-NF matrices presented themselves as having more sensing ability in terms of higher FCER values, this difference is clearly seen in Figures 19-d and 20-d. This is probably due to the greater response of PVA fibers to the connecting with GNP molecules than the latter to nylon fibers. The results obtained from this work are consistent with previous work regarding the sensitivity of samples to applied load over time, where Saafi, et al. [21] demonstrated that the synergistic effect between GNP and fly ash leads to a significant improvement in the development of electrical conductivity by reducing porosity within cementitious composites, where the behavior is linear with respect to the ability of samples to respond to damage by applied tensile load, which is in complete agreement with the behavior of the matrices in this study under tensile loads applied to GNP-PVA and GNP-NF blends. This justification is consistent with Lynch, et al. [72] who concluded that when the concentration of GNP filler is between 1.2 and 3.6% by weight of cementitious materials, the interfaces between the paste and the nanofiller increase, which justifies the high initial sensing values. Then, with increasing stress over time, the microcracks increase by spreading and connecting with each other afterwards, which causes damage to the electrically conductive network and a decrease in the cross-sectional area considered for conductivity. The above explanation suggests that increasing the applied stress causes the sample to gradually deteriorate over time until it fails. This, in turn, leads to the interruption of the conductive network paths formed by the GNP filler due to its separation from the cement paste.

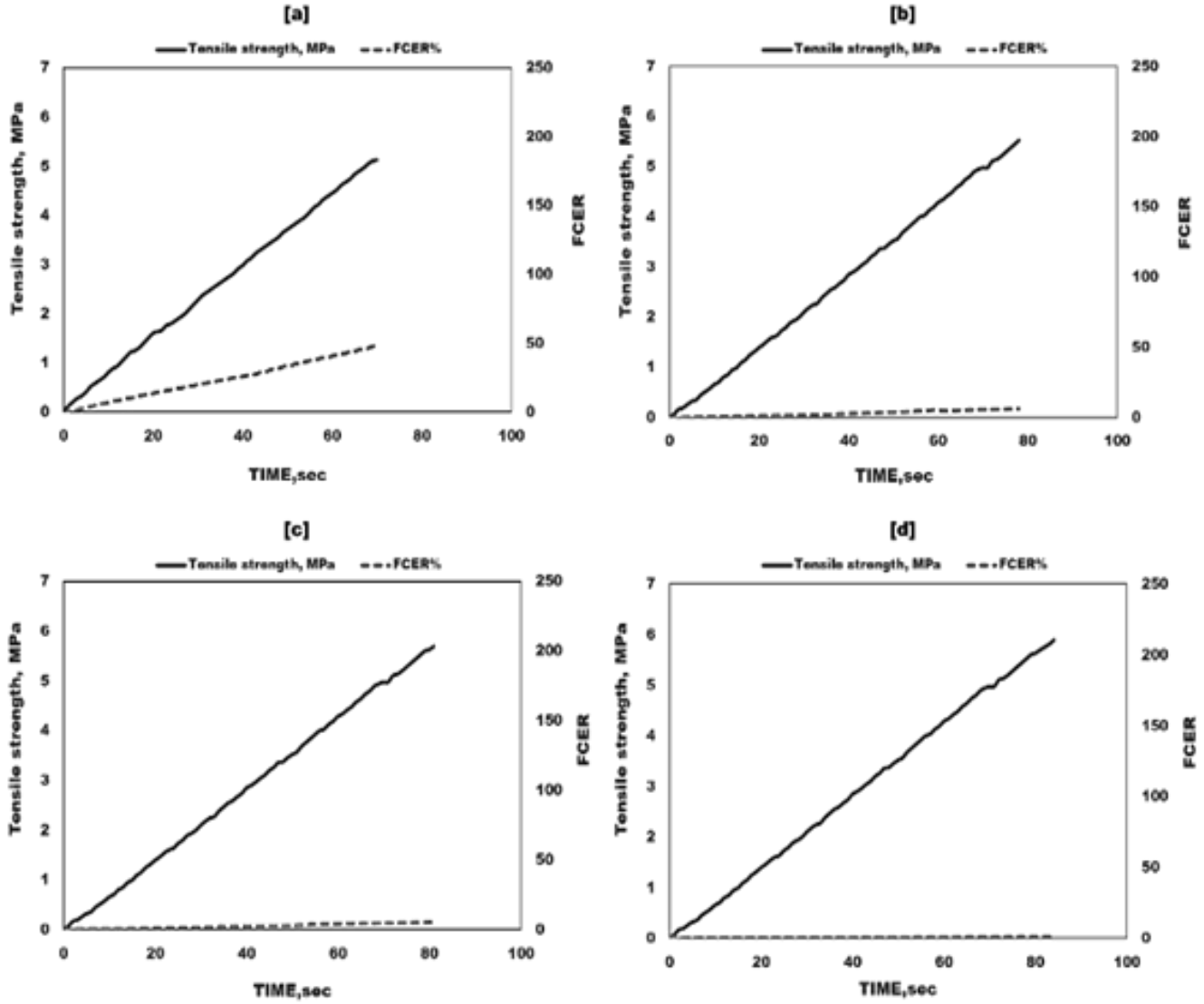

Figure 7: Self-Sensing of reference mixtures under Direct Tensile Strength for different curing age; a)28 days, b)56 days, c) 90 days, and d)180 days

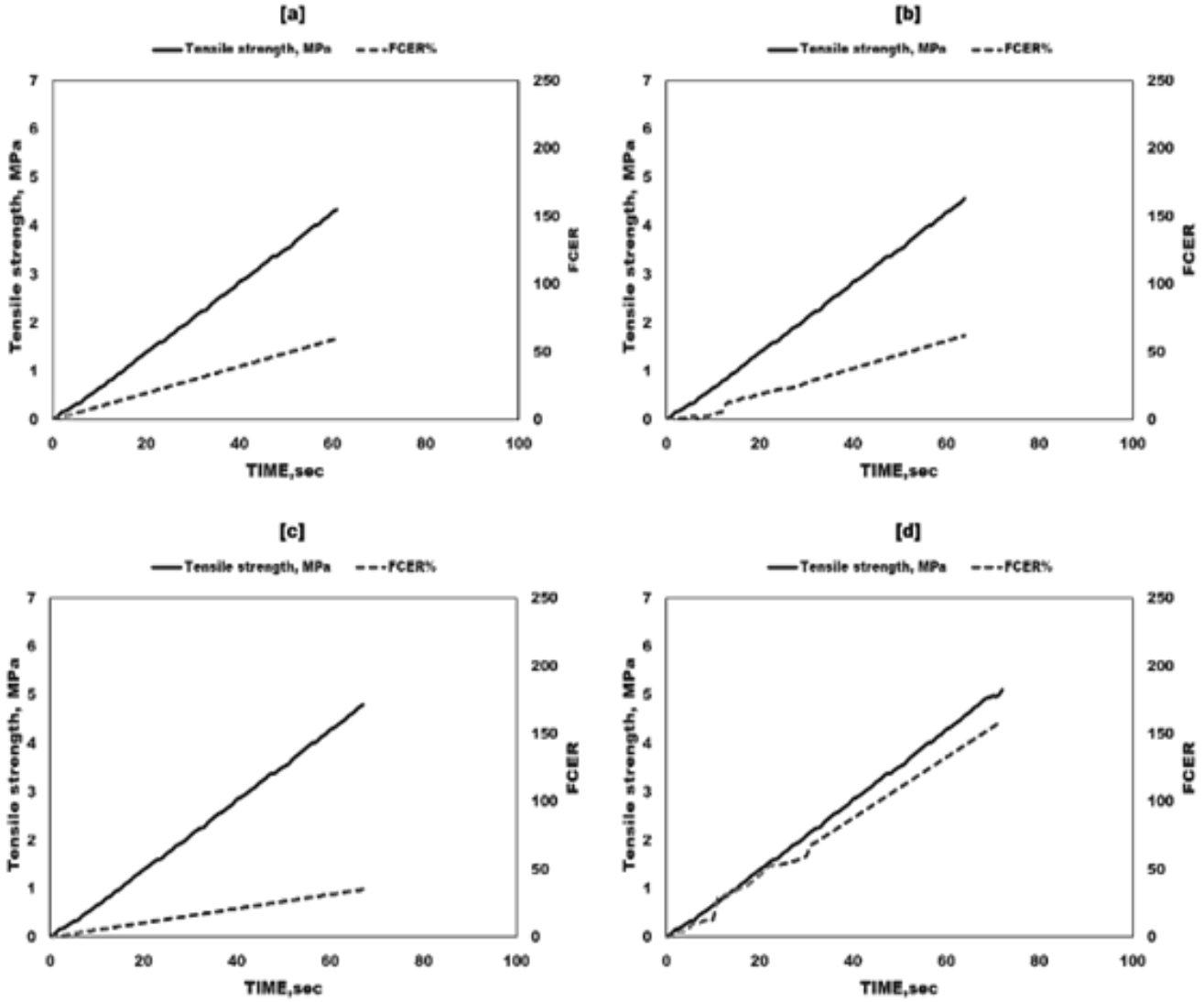

Figure 8: Self-Sensing of GNP-PVA mixtures under Direct Tensile Strength for different curing age; a)28 days, b)56 days, c) 90 days, and d)180 days

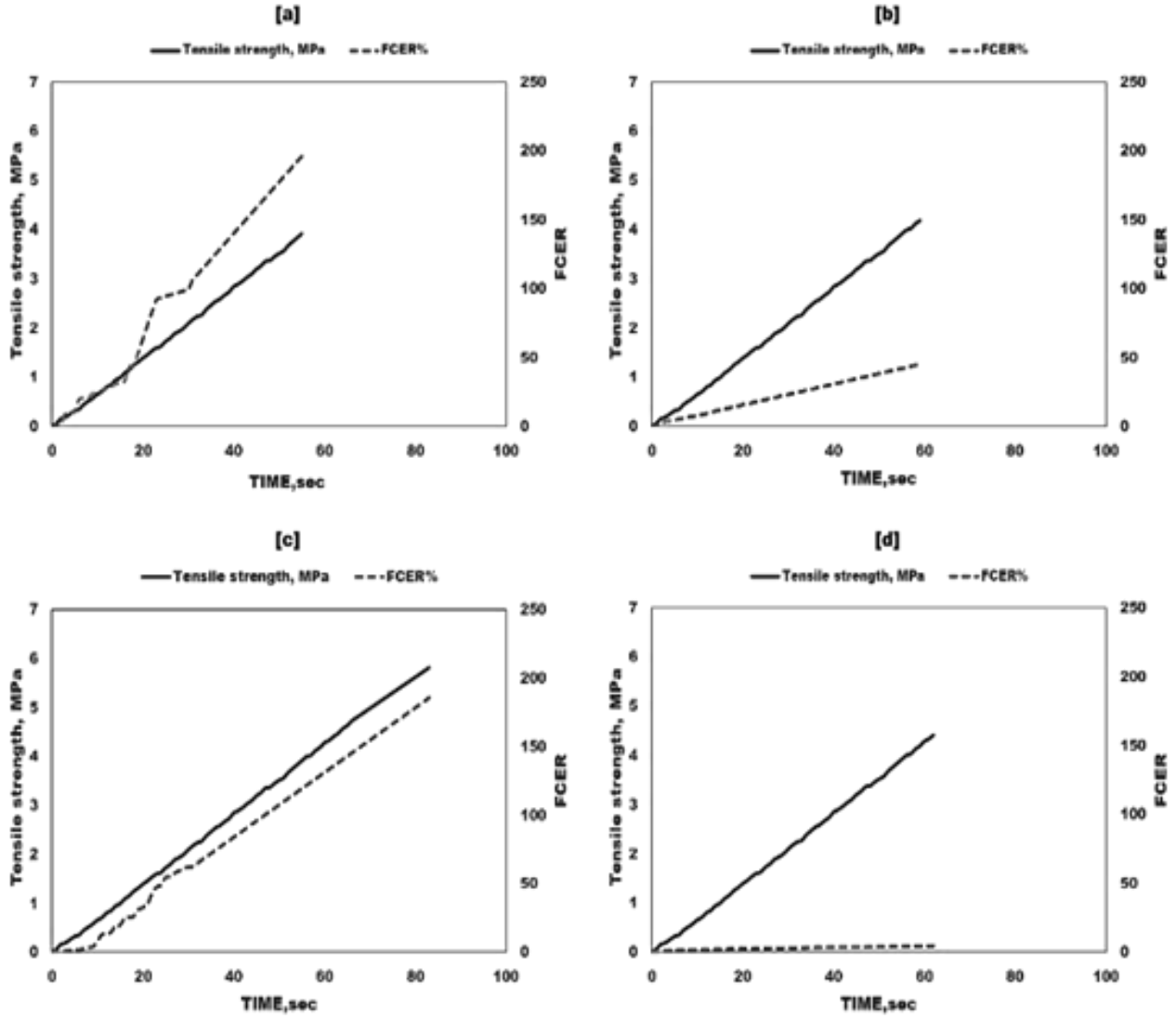

Figure 19: Self-Sensing of GNP-NF mixtures under Direct Tensile Strength for different curing age; a)28 days, b)56 days, c) 90 days, and d)180 days

7. Conclusions

This investigation focuses on understanding the electrical and mechanical behavior of innovative clever composites of plain ECC matrix incorporation with carbon nanofillers (GNP) and reinforced with PVA and NF fibers for curing ages of 28, 56, 90, and 180 days. The laboratory tests applied to the study samples to evaluate the self-sensing ability and durability included monotonic compression strength, direct and indirect tensile strength, and three-point flexural strength. The results obtained in this paper can be summarized as follows:

a. The Regarding the mechanical aspect and in comparison, with the reference mixtures to provide a clearer picture, the synergistic effect of GNP and reinforcing fibers on the strength development of the mixtures is very good to say the least, especially at late ages due to the acceleration and continuation of the hydration processes beyond 28 days. The effect of nanofillers on the mechanical properties was clear in terms of the close bonding with the cement paste interface in addition to its coating of the reinforcing fibers, which improved the adhesion and bonding of the fibers with the cement paste. Moreover, there was a positive effect of the reinforcing fibers (polyvinyl

alcohol and nylon fibers) throughout the study ages and for all the loading scenarios applied in this paper. This distinctive behavior can make these matrices a strong candidate for field works related to civil engineering, such as concrete structures, infrastructure, and rigid pavements.

b. Concerning the functional aspect of these matrices, they showed a unique behavior to our knowledge regarding the evolution of the self-sensing ability of carbon-based nanofiller arrays at late ages, which is contrary to the common behavior of functional arrays where the sensing ability often decreases at late ages due to the gel development that negatively affects the conductive network paths within the array. Furthermore, in general, good FCER values were recordable from the zero point and evolved with the load development for the loading scenarios proposed in this investigation.

Acknowledgment: The researchers would like to thank those who contributed to the completion of this research. Also, thanks are dedicated to the laboratories of the University of Technology in Baghdad – Iraq for their help in conducting the tests adopted in this research.

Conflict of interest: The authors declare that they have no Conflict of interest

Data availability: Data will be made available on request.

References

[1] Abdullah, R. D.; Al-Dahawi, A.; Zghair, H. H. Mechanical Characteristics and Self-Monitoring Technique of Smart Cementitious Mixtures with Carbon Fiber and Graphite Powder as Hybrid Functional Additives. Eng. Technol. J. 40(11), 1537–1547, 2022. https://doi.org/10.30684/etj.2022.134097.1220.

[2] Al-Dahawi, A.; Öztürk, O.; Emami, F.; Yıldırım, G.; Şahmaran, M. Effect of Mixing Methods on the Electrical Properties of Cementitious Composites Incorporating Different Carbon-Based Materials. Constr. Build. Mater. 104, 160–168, 2016. https://doi.org/10.1016/j.conbuildmat.2015.12.072.

[3] Abdullah, R. D.; Al-Dahawi, A. M.; Zghair, H. H. Mechanical and Self-Sensing Properties of Cementitious Composites with Hybrid Carbon Particles/Fibers as Functional Fillers. 4th Int. Sci. Conf. Eng. Sci. Adv. Technol., 2023.

[4] Wang, Y.; Sun, S.; Zhang, L. Self-Sensing Cementitious Composites Incorporating Hybrid NGPs/CNTs/NCBs for Structural Health Monitoring. Sens. Actuat. A Phys. 357, 114365, 2023. https://doi.org/10.1016/j.sna.2023.114365.

[5] Han, B.; Sun, S.; Ding, S.; Zhang, L.; Yu, X.; Ou, J. Review of Nanocarbon-Engineered Multifunctional Cementitious Composites. Compos. Part A Appl. Sci. Manuf. 70, 69–81, 2015. https://doi.org/10.1016/j.compositesa.2014.12.002.

[6] Dong, W.; Li, W.; Tao, Z.; Wang, K. Piezoresistive Properties of Cement-Based Sensors: Review and Perspective. Constr. Build. Mater. 203, 146–163, 2019. https://doi.org/10.1016/j.conbuildmat.2019.01.081.

[7] Kim, G. M.; Nam, I. W.; Yang, B.; Yoon, H. N.; Lee, H. K.; Park, S. Carbon Nanotube (CNT) Incorporated Cementitious Composites for Functional Construction Materials: The State of the Art. Compos. Struct. 227, 111244, 2019. https://doi.org/10.1016/j.compstruct.2019.111244.

[8] Dong, W.; Li, W.; Wang, K.; Shah, S. P. Physicochemical and Piezoresistive Properties of Smart Cementitious Composites with Graphene Nanoplates and Graphite Plates. Constr. Build. Mater. 286, 122943, 2021. https://doi.org/10.1016/j.conbuildmat.2021.122943.

[9] Mahdi, S. A.; et al. Chemical Structure Modification of Polystyrene (PS): A Short Review. Al-Nahrain J. Sci. 27(5), 58–69, 2024. https://doi.org/10.22401/anjs.27.5.07.

[10] Mussa, F.; Al-Dahawi, A.; Banyhussan, Q. S.; Baanoon, M. R.; Shalash, M. A. Carbon Fiber-Reinforced Asphalt Concrete: An Investigation of Some Electrical and Mechanical Properties. IOP Conf. Ser. Mater. Sci. Eng. 737, 012122, 2020. https://doi.org/10.1088/1757-899X/737/1/012122.

[11] Al-Dahawi, A. M.; Mohammed, A.; Banyhussan, Q. S. Effect of Adding Additional Carbon Fiber on Piezoresistive Properties of Fiber Reinforced Concrete Pavements under Impact Load. Eng. Technol. J. 39(12), 1771–1780, 2021. http://doi.org/10.30684/etj.v39i12.1942.

[12] Ghadhban, D.; Joni, H. H.; Al-Dahawi, A. M. Carbon Fiber-Based Cementitious Composites for Traffic Detection and Weighing In Motion.

Eng. Technol. J. 39(8), 1250–1256, 2021. https://doi.org/10.30684/etj.v39i8.1875.
[13] Hameed, I. T.; Al-Dahawi, A. Electro-Mechanical Properties of Functional Fiber-Based Rigid Pavement under Various Loads Applied on a Large-Scale In-Situ Section. E3S Web Conf. 427, 03033, 2023. https://doi.org/10.1051/e3sconf/202342703033.
[14] Chung, D. D. L. Carbon Materials for Structural Self-Sensing, Electromagnetic Shielding and Thermal Interfacing. Carbon 50(9), 3342–3353, 2012. https://doi.org/10.1016/j.carbon.2012.01.031.
[15] Xu, G.; Du, S.; He, J.; Shi, X. The Role of Admixed Graphene Oxide in a Cement Hydration System. Carbon 148, 141–150, 2019. https://doi.org/10.1016/j.carbon.2019.03.072.
[16] Hasan, A. A.; Al-Mashhadani, M. H.; Al-Dahhan, W. H.; Yusop, R. M.; Yousif, E. A. Recent Approaches to Modify Poly(vinyl chloride) Chemical Structure. Al-Nahrain J. Sci. 25(3), 8–15, 2022. https://doi.org/10.22401/anjs.25.3.02.
[17] Li, W.; Dong, W.; Shen, L.; Castel, A.; Shah, S. P. Conductivity and Piezoresistivity of Nano-Carbon Black (NCB) Enhanced Functional Cement-Based Sensors Using Polypropylene Fibres. Mater. Lett. 270, 127736, 2020. https://doi.org/10.1016/j.matlet.2020.127736.
[18] Yang, H.; Cui, H.; Tang, W.; Li, Z.; Han, N.; Xing, F. A Critical Review on Research Progress of Graphene/Cement Based Composites. Compos. Part A Appl. Sci. Manuf. 102, 273–296, 2017. https://doi.org/10.1016/j.compositesa.2017.07.019.
[19] Sedaghat, A.; Ram, M. K.; Zayed, A.; Kamal, R.; Shanahan, N. Investigation of Physical Properties of Graphene-Cement Composite for Structural Applications. Open J. Compos. Mater. 4(1), 12–21, 2014. https://doi.org/10.4236/ojcm.2014.41002.
[20] Pang, S. D.; Gao, H. J.; Xu, C.; Quek, S. T.; Du, H. Strain and Damage Self-Sensing Cement Composites with Conductive Graphene Nanoplatelet. In Sensors and Smart Structures Technologies for Civil, Mechanical, and Aerospace Systems 2014; SPIE: Bellingham, WA, USA, 2014; Vol. 9061, pp. 546–556.
[21] Saafi, M.; et al. Graphene/Fly Ash Geopolymeric Composites as Self-Sensing Structural Materials. Smart Mater. Struct. 23, 065006, 2014. https://doi.org/10.1088/0964-1726/23/6/065006.
[22] Chuah, S.; Pan, Z.; Sanjayan, J. G.; Wang, C. M.; Duan, W. H. Nano Reinforced Cement and Concrete Composites and New Perspective from Graphene Oxide. Constr. Build. Mater. 73, 113–124, 2014. https://doi.org/10.1016/j.conbuildmat.2014.09.040.
[23] Iraqi Standard Specification. Iraqi Standard Specification No. 5, for Portland Cement; Central Organization for Standardization and Quality: Iraq, 1984.
[24] ASTM-C618. Standard Specification for Coal Fly Ash and Raw or Calcined Natural Pozzolan for Use in Concrete; ASTM Int.: West Conshohocken, PA, USA, 2014; https://doi.org/10.1520/c0618-12a.
[25] ASTM C494/C494M. Standard Specification for Chemical Admixtures for Concrete. Annu. Book ASTM Stand. 2019, 04.
[26] Abdullah, R.; Al-Dahawi, A.; Zghair, H. Mechanical Characteristics and Self-Monitoring Technique of Smart Cementitious Mixtures with Carbon Fiber and Graphite Powder as Hybrid Functional Additives. Eng. Technol. J. 40(11), 1537–1547, 2022. http://doi.org/10.30684/etj.2022.134097.1220.
[27] Abdullah, R. D. Mechanical and Self-Sensing Properties of Cementitious Pavement Composites Enhanced with Hybrid Electrically Conductive Materials; University of Technology: 2022.
[28] Al-Dahawi, A. M.; Abdullah, R. D.; Joni, H. H. An Investigation of Self-Sensing and Mechanical Properties of Smart Engineered Cementitious Composites Reinforced with Functional Materials. Open Eng. 14(1), 2024. https://doi.org/10.1515/eng-2022-0568.
[29] Al-Dahawi, A. M. Effect of Curing Age on the Self-Sensing Behavior of Carbon-Based Engineered Cementitious Composites (ECC) under Monotonic Flexural Loading Scenario. MATEC Web Conf. 162, 2018. https://doi.org/10.1051/matecconf/201816201034.
[30] Sarwary, M. H.; et al. Self-Sensing of Flexural Damage in Large-Scale Steel-Reinforced Mortar Beams. ACI Mater. J. 116(4), 2019. https://doi.org/10.14359/51715581.
[31] Yıldırım, G.; Öztürk, O.; Al-Dahawi, A.; Ulu, A. A.; Şahmaran, M. Self-Sensing Capability of Engineered Cementitious Composites: Effects of Aging and Loading Conditions. Constr. Build. Mater. 231, 2020.

https://doi.org/10.1016/j.conbuildmat.2019.117132.
[32] Şahmaran, M.; Li, V. C. Durability of Mechanically Loaded Engineered Cementitious Composites under Highly Alkaline Environments. Cem. Concr. Compos. 30(2), 72–81, 2008. https://doi.org/10.1016/j.cemconcomp.2007.09.004.
[33] Sahmaran, M.; Yildirim, G.; Erdem, T. K. Self-Healing Capability of Cementitious Composites Incorporating Different Supplementary Cementitious Materials. Cem. Concr. Compos. 35(1), 89–101, 2013. https://doi.org/10.1016/j.cemconcomp.2012.08.013.
[34] ASTM-C109/C109M. Standard Test Method for Compressive Strength of Hydraulic Cement Mortars (Using 2-in. or [50-mm] Cube Specimens); ASTM Int.: West Conshohocken, PA, USA, 2005.
[35] ASTM-C496–96. Standard Test Method for Splitting Tensile Strength of Cylindrical Concrete Specimens; ASTM Int.: West Conshohocken, PA, USA, 2017. https://doi.org/10.1520/C0496-96.
[36] ASTM-C348–02. Standard Test Method for Flexural Strength of Hydraulic-Cement Mortars; ASTM Int.: West Conshohocken, PA, USA, 2002.
[37] ASTM-C307−03. Standard Test Method for Tensile Strength of Chemical-Resistant Mortar, Grouts, and Monolithic Surfacings; ASTM Int.: West Conshohocken, PA, USA, 2012. https://doi.org/10.1520/c0307-03r12.
[38] Al-Dahawi, A.; et al. Electrical Percolation Threshold of Cementitious Composites Possessing Self-Sensing Functionality Incorporating Different Carbon-Based Materials. Smart Mater. Struct. 25(10), 2016. http://dx.doi.org/10.1088/0964-1726/25/10/105005.
[39] Al-Dahawi, A.; Yıldırım, G.; Öztürk, O.; Şahmaran, M. Assessment of Self-Sensing Capability of Engineered Cementitious Composites within the Elastic and Plastic Ranges of Cyclic Flexural Loading. Constr. Build. Mater. 145, 1–10, 2017. https://doi.org/10.1016/j.conbuildmat.2017.03.236.
[40] Wen, S.; Chung, D. D. L. Piezoresistivity in Continuous Carbon Fiber Cement-Matrix Composite. Cem. Concr. Res., 1999.
[41] Fernando, L.; Pemasiri, K.; Dassanayake, B. Combined Effects of Rice Husk Ash and Nylon Fiber on Engineering Properties of Cement Mortar. SN Appl. Sci. 2(3), 2020. https://doi.org/10.1007/s42452-020-2198-1.
[42] Aslani, F.; Nejadi, S. Bond Characteristics of Steel Fiber and Deformed Reinforcing Steel Bar Embedded in Steel Fiber Reinforced Self-Compacting Concrete (SFRSCC). Cent. Eur. J. Eng. 2012. https://doi.org/10.2478/s13531-012-0015-3.
[43] Hamedanimojarrad, P.; Adam, G.; Ray, A.; Thomas, P.; Vessalas, K. Development of Shrinkage Resistant Microfibre-Reinforced Cement-Based Composites. Open Eng. 2(2), 2012. https://doi.org/10.2478/s13531-011-0065-y.
[44] Han, B.; Ding, S.; Yu, X. Intrinsic Self-Sensing Concrete and Structures: A Review. Measurement 59, 110–128, 2015. https://doi.org/10.1016/j.measurement.2014.09.048.
[45] Habib, A.; Alam, M. Mechanical Properties of Synthetic Fibers Reinforced Mortars. Int. J. Sci. Eng. Res. 4(4), 2013.
[46] Huang, Y.; Li, H.; Qian, S. Self-Sensing Properties of Engineered Cementitious Composites. Constr. Build. Mater. 174, 253–262, 2018. https://doi.org/10.1016/j.conbuildmat.2018.04.129.
[47] Bheel, N.; Mohammed, B. S.; Ali, M. O. A.; Shafiq, N.; Radu, D. Effect of Graphene Oxide as a Nanomaterial on the Bond Behaviour of Engineered Cementitious Composites by Applying RSM Modelling and Optimization. J. Mater. Res. Technol. 26, 1484–1507, 2023. https://doi.org/10.1016/j.jmrt.2023.07.278.
[48] Ahmad, J.; Zaid, O.; Pérez, C. L.-C.; Martínez-García, R.; López-Gayarre, F. Experimental Research on Mechanical and Permeability Properties of Nylon Fiber Reinforced Recycled Aggregate Concrete with Mineral Admixture. Appl. Sci. 12(2), 2022. https://doi.org/10.3390/app12020554.
[49] Lv, S.; Ma, Y.; Qiu, C.; Sun, T.; Liu, J.; Zhou, Q. Effect of Graphene Oxide Nanosheets on Microstructure and Mechanical Properties of Cement Composites. Constr. Build. Mater. 49, 121–127, 2013. https://doi.org/10.1016/j.conbuildmat.2013.08.022.
[50] Yoo, D.-Y.; Kim, S.; Lee, S. H. Self-Sensing Capability of Ultra-High-Performance Concrete

Containing Steel Fibers and Carbon Nanotubes under Tension. Sens. Actuat. A Phys. 276, 125–136, 2018. https://doi.org/10.1016/j.sna.2018.04.009.

[51] Lee, S. H.; Kim, S.; Yoo, D.-Y. Hybrid Effects of Steel Fiber and Carbon Nanotube on Self-Sensing Capability of Ultra-High-Performance Concrete. Constr. Build. Mater. 185, 530–544, 2018. https://doi.org/10.1016/j.conbuildmat.2018.07.071.

[52] Yao, X.; Huang, G.; Wang, M.; Dong, X. Mechanical Properties and Microstructure of PVA Fiber Reinforced Cemented Soil. KSCE J. Civ. Eng. 25(2), 482–491, 2020. https://doi.org/10.1007/s12205-020-0998-x.

[53] Hawreen, A.; Bogas, J. A.; Dias, A. P. S. On the Mechanical and Shrinkage Behavior of Cement Mortars Reinforced with Carbon Nanotubes. Constr. Build. Mater. 168, 459–470, 2018. https://doi.org/10.1016/j.conbuildmat.2018.02.146.

[54] Hawreen, A.; Bogas, J. A.; Kurda, R. Mechanical Characterization of Concrete Reinforced with Different Types of Carbon Nanotubes. Arab. J. Sci. Eng. 44(10), 8361–8376, 2019. https://doi.org/10.1007/s13369-019-04096-y.

[55] Wu, Y. Y.; Zhang, J.; Liu, C.; Zheng, Z.; Lambert, P. Effect of Graphene Oxide Nanosheets on Physical Properties of Ultra-High-Performance Concrete with High Volume Supplementary Cementitious Materials. Materials (Basel) 13(8), 1929, 2020. https://doi.org/10.3390/ma13081929.

[56] Shamsaei, E.; de Souza, F. B.; Yao, X.; Benhelal, E.; Akbari, A.; Duan, W. Graphene-Based Nanosheets for Stronger and More Durable Concrete: A Review. Constr. Build. Mater. 183, 642–660, 2018. https://doi.org/10.1016/j.conbuildmat.2018.06.201.

[57] Dang, C. T.; Pham, M.; Dinh, N. H. Experimental Study on Compressive and Flexural Performance of Lightweight Cement-Based Composites Reinforced with Hybrid Short Fibers. Materials (Basel) 16(12), 4457, 2023. https://doi.org/10.3390/ma16124457.

[58] Mohsen, M. O.; Al Ansari, M. S.; Taha, R.; Al Nuaimi, N.; Taqa, A. A. Carbon Nanotube Effect on the Ductility, Flexural Strength, and Permeability of Concrete. J. Nanomater. 2019, 6490984, 2019. https://doi.org/10.1155/2019/6490984.

[59] Ranade, R.; Zhang, J.; Lynch, J. P.; Li, V. C. Influence of Micro-cracking on the Composite Resistivity of Engineered Cementitious Composites. Cem. Concr. Res. 58, 1–12, 2014. http://dx.doi.org/10.1016/j.cemconres.2014.01.002.

[60] Rovnaník, P.; Kusák, I.; Schmid, P. Self-Sensing Properties of Fly Ash Geopolymer Composite with Graphite Filler. In Spec. Conc. Compos. 2020, 17th Int. Conf., 2021.

[61] Si, T.; et al. Synergistic Effects of Carbon Black and Steel Fibers on Electromagnetic Wave Shielding and Mechanical Properties of Graphite/Cement Composites. J. Build. Eng. 45, 103561, 2022. https://doi.org/10.1016/j.jobe.2021.103561.

[62] Reza, F.; Batson, G. B.; Yamamuro, J. A.; Lee, J. S. Resistance Changes during Compression of Carbon Fiber Cement Composites. Mater. Civ. Eng. 15(5), 2003. https://doi.org/10.1061/(ASCE)0899-1561(2003)15:5(476).

[63] Yildirim, G.; Aras, G. H.; Banyhussan, Q. S.; Şahmaran, M.; Lachemi, M. Estimating the Self-Healing Capability of Cementitious Composites through Non-Destructive Electrical-Based Monitoring. NDT E Int. 76, 26–37, 2015. https://doi.org/10.1016/j.ndteint.2015.08.005.

[64] Li, M.; Lin, V.; Lynch, J.; Li, V. C. Multifunctional Carbon Black Engineered Cementitious Composites for the Protection of Critical Infrastructure. High Perform. Fiber Reinforc. Cem. Compos. 6, 99–106, 2012. https://doi.org/10.1007/978-94-007-2436-5_13.

[65] Roshan, M. J.; Abedi, M.; Gomes Correia, A.; Fangueiro, R. Application of Self-Sensing Cement-Stabilized Sand for Damage Detection. Constr. Build. Mater. 403, 133080, 2023. https://doi.org/10.1016/j.conbuildmat.2023.133080.

[66] Yoo, D.-Y.; You, I.; Lee, S.-J. Electrical and Piezoresistive Sensing Capacities of Cement Paste with Multi-Walled Carbon Nanotubes. Arch. Civ. Mech. Eng. 18(2), 371–384, 2018. https://doi.org/10.1016/j.acme.2017.09.007.

[67] Suchorzewski, J.; Prieto, M.; Mueller, U. An Experimental Study of Self-Sensing Concrete Enhanced with Multi-Wall Carbon Nanotubes in Wedge Splitting Test and DIC. Constr. Build. Mater. 262, 120871, 2020. https://doi.org/10.1016/j.conbuildmat.2020.120871.

[68] Wang, D.; Wang, S.; Chung, D.; Chung, J. Comparison of the Electrical Resistance and Potential Techniques for the Self-Sensing of Damage in Carbon Fiber Polymer-Matrix Composites. J. Intell. Mater. Syst. Struct. 17, 2006. https://doi.org/10.1177/1045389X06060218.
[69] Hou, T.-C.; Lynch, J. Conductivity-Based Strain Monitoring and Damage Characterization of Fiber Reinforced Cementitious Structural Components. Proc. SPIE Int. Soc. Opt. Eng. 5765, 2005. https://doi.org/10.1117/12.599955.
[70] Saafi, M. Wireless and Embedded Carbon Nanotube Networks for Damage Detection in Concrete Structures. Nanotechnology 20, 395502, 2009. https://doi.org/10.1088/0957-4484/20/39/395502.
[71] Chan, Y.-W.; Chu, S.-H. Effect of Silica Fume on Steel Fiber Bond Characteristics in Reactive Powder Concrete. Cem. Concr. Res. 34(7), 1167–1172, 2004. https://doi.org/10.1016/j.cemconres.2003.12.023.
[72] Lynch, J. P.; et al. Strain and Damage Self-Sensing Cement Composites with Conductive Graphene Nanoplatelet. Sensors and Smart Structures Technologies for Civil, Mechanical, and Aerospace Systems 2014, 2014.